Aalborg Universitet

AALBORG UNIVERSITY
DENMARK

Active Vibration Control of Civil Engineering Structures under Earthquake Excitation

Thesbjerg, L.

Publication date:
1990

Document Version
Early version, also known as pre-print

[Link to publication from Aalborg University](#)

Citation for published version (APA):
Thesbjerg, L. (1990). *Active Vibration Control of Civil Engineering Structures under Earthquake Excitation*. Dept. of Building Technology and Structural Engineering, Aalborg University. Fracture and Dynamics Vol. R9027 No. 25

FRACTURE & DYNAMICS

PAPER NO. 25

FRACTURE & DYNAMICS

PAPER NO. 25

Contents

Preface

This report *Active Vibration Control of Civil Engineering Structures under Earthquake Excitation* is the result of theoretical and experimental investigations at the Department of Building Technology and Structural Engineering, University of Aalborg.

The experiment was performed in cooperation with Mr. C. Ladefoged and Ms. A. D. Karstensen, final year students, in connection with their M.Sc.-Thesis at the University of Aalborg. Their assistance is greatly appreciated.

Aalborg, August 1990   Leo Thesbjerg

Chapter 1

Introduction

Structures are exposed to dynamic loadings from several sources, for instance earthquake ground motion, wind gusts and severe sea states. Further to these natural actions moving vehicles and other machines may also cause dynamic excitation.

When a structure is designed different arrangements can be made to take into account the dynamic actions. One method of solution is to dimension the structure in such a way that it can resist the dynamic actions. Another is obtained by making arrangements which can reduce the response of the structure. The last-mentioned techniques may be split up into two main groups :

1. Passive vibration suppression

2. Active vibration suppression

Considering civil engineering structures the design objectives have always been to obtain an adequate safety of the structure, which during several centuries has been obtained by making the dimensions of the different parts sufficiently large. Passive vibration suppression for providing structural safety was seriously considered more than 50 years ago. At that time the technique of creating a so- called "flexible first-storey" of a multistorey building was suggested. If properly designed a flexibility of the first storey will provide an isolation effect against large dynamic shear forces during earthquakes. Later the concept has not been generally accepted because of an inherently large lateral motion required.

Recent research efforts have focused on a variety of base isolation systems as potential improvements over the soft first-storey concept. One of the simplest concepts is to mount the structure on horizontal pads which permit lateral slip between the base of the structure and its foundation. These bearing pads may for instance be constructed as a sandwich of a large number of alternating thin plates of steel and natural rubber.

Another arrangement used in attenuating the response of earthquake-excited structures is the conventional linear auxiliary mass damper.

The above-mentioned techniques for passive vibration suppression are sometimes designated vibration isolation, because in principle there is no energy dissipation. However, passive vibration suppression may also be due to absorption of mechanical energy from the structure which for instance relies on dissipation in the material, interface slip between adjacent elements or plastic deformations, etc. The efficiency of the natural passive energy absorption can be improved by putting on conventional passive viscous dampers.

Vibration isolators are only effective if the dominating frequencies in the spectrum of the dynamic loading belong to fixed intervals. Therefore, in case of considerable uncertainty

in defining the dynamic loading, and if the loading is of a broad-banded character the passive control systems may be inadequate.

Driven by economic disincentives such as increasing relative costs for materials and by increasing economic viability of sophisticated analysis techniques the minimum weight condition has become an important design requirement for many dynamically loaded civil engineering structures and thereby, they are built increasingly more slender and flexible. This, in turn, can lead to excessive vibrations which may need to be suppressed to prevent the structure from oscillating beyond acceptable limits. On account of this and the limitations in passive control automatic controls have been considered.

The prime objective of introducing active control to civil engineering structures is to ensure their safety, which is usually governed by its response to an infrequent event such as a severe earthquake. As a result, an active earthquake control system would have to remain in standby mode for many years and perhaps several decades without being activated. The reliability of infrequently used equipment then becomes a serious liability. An additional concern for active control systems is that the time at which the control power is most needed often coincides with the time at which failure of most utility systems can be expected. For these and other reasons attention still has to be given to passive control measures, but because of the evident possibilities reasonable efforts for active control devices are still required.

A few tall buildings have already been built with automatic vibration suppression. The actuators installed are mostly active tuned mass dampers, whose primary function is to reduce wind-induced vibration in a few prominent modes, and they have operated satisfactorily. An alternative control mechanism for active control of tall buildings is the active tendons. The applicability of this system has been examined by experiments on laboratory models subjected to base motions simulating seismic frame buildings, [1, 2]. Theoretically, both control systems for reduction of adverse effects of earthquake and wind have been studied, using different control schemes showing varying degrees of efficiency [3,4,5,6,7].

Active feedback control of large and massive civil engineering structures is of relatively recent vintage, but it has been prominent in the aerospace, electrical, and mechanical engineering fields. Many of the issues are the same, i.e. such topics as mathematical modelling of structures, identification techniques, reduced-order models, modal truncation and controller interaction with residual modes, placement of controller and optimal control techniques.

In active control of civil structures the most common methods for determining the feedback gains of the control signal are based on the optimal control techniques. These methods are concerned with designing a system which is the best possible with respect to a standard. While determining the feedback gains, the objective is to minimize a suitable objective function describing the level of the vibration and the control forces. This optimal control problem has been treated in many papers, considering a variety of structures described by different mathematical models. Using distributed parameter models the optimal control system has been designed for a beam with constant cross-section [8] and with variable cross-section [9], a plate [10] and a membrane [11].

Structures can generally be represented by distributed-parameter systems, but considering large structures it is normally necessary to use a discrete model, since optimal control of large distributed-parameter systems poses mathematical and design problems of considerable difficulty. The structural system can be discretized either by a finite element

scheme or a finite difference scheme. In both cases the equations of motion are reduced to ordinary, coupled differential equations. The resulting discrete model generally possesses a large number of degrees of freedom. Designing an optimal feedback control law is then a very difficult and time-consuming process.

As an approach the control scheme of independent modal space control is introduced, which has been extensively developed by Meirovitch et al. [12,13]. In this method it is assumed, that the coupled system of equations of motion can be decoupled by a modal approach. Thus the controller is designed for each mode independently of other modes of vibration and, consequently, the computational burden for determining state feedback coefficients is considerably reduced. The control scheme of independent modal space control has formed the basis of several other papers on the application of active control devices [2,7,14,15,16].

The majority of the various control algorithms and control systems being proposed and investigated, have been documented by analytical and simulation results. Further to these results an extensive experimental study is necessary before any application could be adopted. The practical problems include effects of time delay in data acquisition and on-line calculation, unsynchronized application of control forces, interface between controllers and structure, and interface between sensors and structure. Few studies deal with experiments and they mainly deal with the effect of time delay [1,7].

Encouraged by the many, still unanswered questions concerning active vibration control of civil engineering structures this project was initiated.

The object is to study the feasibility of active control of structures under seismic excitation. An optimal closed-loop control scheme using a quadratic performance index is developed for a discretized and a reduced-order model under earthquake excitation. Considering a reduced-order model just a few of the predominant modes are controlled leading to the independent modal space control device. The control law is first set up for the continuous time system, and next for the discrete time system including the effect of time delay between measurement and the application of control forces.

Structural control experiments are carried out in the laboratory using a model structure. The control experiments are performed using an active mass damper and closed-loop modal control algorithms. The model is controlled by free vibrations and by forced vibrations caused by a harmonic base excitation. Results of the experiments clearly show that the closed-loop modal control algorithm can be implemented.æ

Chapter 2

Optimal Control of Discretized and Reduced Order Systems

The purpose is to design a control system, which will be able to attenuate the vibrations of a structure under seismic excitation. It will be designed according to the optimal control techniques.

In order to design an optimal control system an equation of motion for the structure is required. In the light of the equation of motion for a linear elastic distributed parameter system the optimal control system for the associated discretized system will be designed first and then the device of independent modal space control is introduced. By using independent modal space control the so-called spillover effects occur, because it is not possible to observe and control all modes. On the other hand this technique provides relatively few calculations during control.

2.1 Equations of Motion

2.1.1 Distributed Parameter System

The equation of motion for a 3-dimensional linear elastic, distributed parameter system subjected to a time-varying displacement of the base, and under active control, can be described by the following partial differential equation

$$Lu_i \; + \; c(\mathbf{x})\frac{\partial u_i}{\partial t} \; + \; \rho(\mathbf{x})\frac{\partial^2 u_i}{\partial t^2} \; = \; c(\mathbf{x})\frac{\partial}{\partial t}U_i^{(0)}(\mathbf{x},t) \; + \; f_i(\mathbf{x},t) \quad ,$$
$$\forall \, (\mathbf{x},t) \; \in \; \Omega \times \,]0,\infty[\tag{2.1}$$

In (2.1) and below the index summation conventions will be applied to the indices i,j. Eq. (2.1) must be satisfied at every point $\mathbf{x}$ of the domain Ω denoting the structure. $u_i = u_i(\mathbf{x},t)$ is the absolute displacement of an arbitrary point $\mathbf{x}$, L is a linear differential self-adjoint operator of order 2, expressing the stiffness, $c(\mathbf{x})$ and $\rho(\mathbf{x})$ are the distributed linear viscous damping and mass, and $f_i(\mathbf{x},t)$ are distributed control forces. $U_i^{(0)}(\mathbf{x},t)$ is assumed to be the quasi-static displacement caused by the base motion.

The displacement $u_i(\mathbf{x},t)$ is subjected to mechanical boundary conditions at the surface Γ_1 of the structure

$$B_1 u_i \; = \; 0 \quad , \quad \forall \, (\mathbf{x},t) \; \in \; \Gamma_1 \times \,]0,\infty[\tag{2.2}$$

and geometrical boundary conditions at the surface Γ_2

$$u_i(\mathbf{x},t) \; = \; u_{0i}(t) \quad , \quad \forall \, (\mathbf{x},t) \; \in \; \Gamma_2 \times \,]0,\infty[\tag{2.3}$$

where $u_{0i}(t)$ describes the displacement of the base. In eq. (2.2) B_1 is a differential operator of order 1.

The initial conditions at $t = 0$ are

$$u_i(\mathbf{x},0) = 0 \quad , \quad \dot{u}_i(\mathbf{x},0) = 0 \quad , \quad \forall\, \mathbf{x} \in \Omega \times \Gamma_1 \tag{2.4}$$

$U_i^{(0)}(\mathbf{x},t)$ is subjected to the boundary conditions

$$LU_i^{(0)} = 0 \quad , \quad \forall\, (\mathbf{x},t) \in \Omega \times \,]0,\infty[\tag{2.5}$$

$$B_1 U_i^{(0)} = 0 \quad , \quad \forall\, (\mathbf{x},t) \in \Gamma_1 \times \,]0,\infty[\tag{2.6}$$

$$U_i^{(0)}(\mathbf{x},t) = u_{0i}(t) \quad , \quad \forall\, (\mathbf{x},t) \in \Gamma_2 \times \,]0,\infty[\tag{2.7}$$

$U_i^{(0)}$ fulfils arbitrary initial conditions at time $t = 0$.

In practice actuators tend to be discrete elements $F_1(t), F_2(t), ..., F_{n_m}(t)$, where $F_\alpha(t)$ is the control force at the location $\mathbf{x}_\alpha^T = [x_{\alpha 1}, x_{\alpha 2}, x_{\alpha 3}]$ in a direction determined by the unit vector $\mathbf{e}_\alpha^T = [e_{\alpha 1}, e_{\alpha 2}, e_{\alpha 3}]$, i.e.

$$f_i(\mathbf{x},t) = \sum_{\alpha=1}^{n_m} \delta(\mathbf{x} - \mathbf{x}_\alpha) e_{\alpha i} F_\alpha(t) \tag{2.8}$$

where $\delta(\mathbf{x} - \mathbf{x}_\alpha) = \delta(x_1 - x_{\alpha 1})\delta(x_2 - x_{\alpha 2})\delta(x_3 - x_{\alpha 3})$ is a spatial Dirac delta function.

2.1.2 Discrete Parameter System

Basicly, structures are distributed parameter systems and so their equation of motion must be described by the partial differential equations (2.1). Performing optimal control it is necessary to solve these equations of motion and this might be a quite complicated problem for large structures. Hence, to simplify the solution a discretized model can be introduced, so that the structural equations of motion are reduced to ordinary differential equations.

In this section the equations of motion are set up for a discretized system, which for instance could look like the model in fig. 2.1.

The differential operator L in (2.1) can be discretized either by a finite element scheme or by a finite difference scheme. In both cases the boundary - and initial value problem (2.1) - (2.4) is transformed into a system of ordinary differential equations. Using (2.8), this yields

$$\mathbf{M}\ddot{\mathbf{u}} + \mathbf{C}\dot{\mathbf{u}} + \mathbf{K}\mathbf{u} = \mathbf{C}\dot{\mathbf{U}}^{(0)} + \mathbf{K}\mathbf{U}^{(0)} + \mathbf{I}_1\mathbf{F}(t) \quad , \quad t > 0 \tag{2.9}$$
$$\mathbf{u}(0) = \mathbf{0} \;,\; \dot{\mathbf{u}}(0) = \mathbf{0}$$

$\mathbf{u}$ is an n-dimensional vector of the absolute displacements and rotations in the n degrees of freedom of the structure.

The structure is at rest at time $t = 0$. $\mathbf{U}^{(0)}$ specifies the quasi-static displacements and rotations in proportion to the reference configuration caused by the base motion.

$\mathbf{M}$, $\mathbf{C}$ and $\mathbf{K}$ signify mass, damping, and stiffness matrices, respectively, all of dimension $n \times n$. $\mathbf{M}$ and $\mathbf{K}$ are symmetrical due to the Maxwell-Betti reciprocal theorem of linear elasticity. $\mathbf{M}$ is positive semi-definite whereas $\mathbf{K}$ is positive definite. $\mathbf{C}$ is generally non-symmetric and is positive definite for any dissipative system.
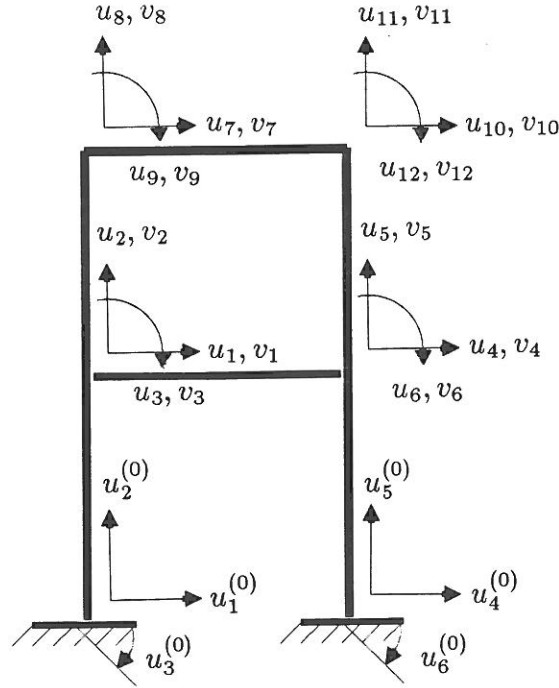
Figure 2.1: Plane linear elastic frame with a movable base. Definition of absolute and relative displacement.

$\mathbf{F}^T(t) = [F_1(t), ..., F_{n_m}(t)]$ is an n_m-dimensional vector of control forces $F_\alpha(t)$ applied at the point $\mathbf{x}_\alpha$ in the direction determined by the unit vector $\mathbf{e}_\alpha$.

$\mathbf{I}_1$ is a constant influence matrix of dimension $n \times n_m$. Column α states the nodal loading in the degrees of freedom $\mathbf{u}$, when a unit force is applied at point $\mathbf{x}_\alpha$ in the direction $\mathbf{e}_\alpha$.

$\mathbf{u}^{(0)T}(t) = [u_1^{(0)}(t), ..., u_l^{(0)}(t)]$ is an l-dimensional vector of nodal motions at the base. As it is shown in fig. 2.1 $\mathbf{u}^{(0)}(t)$ both contain translations and rotations.

$\mathbf{U}^{(0)}(t)$ is caused by the time-varying base motions $\mathbf{u}^{(0)}(t)$. On account of the linearity, we have

$$\mathbf{U}^{(0)}(t) = \mathbf{I}_2 \mathbf{u}^{(0)}(t) \tag{2.10}$$

$\mathbf{I}_2$ is a constant influence matrix of dimension $n \times l$. Column i states the displacement in the degrees of freedom $\mathbf{u}$, when $u_i^{(0)}$ is equal to 1, and the remaining components is equal to 0. $\mathbf{I}_2$ is determined by statical methods.

The relative displacement $\mathbf{v}(t)$ with respect to the quasi-static displacement $\mathbf{U}^{(0)}(t)$ is given by

$$\mathbf{v}(t) = \mathbf{u}(t) - \mathbf{U}^{(0)}(t) \tag{2.11}$$

Substituting (2.10) and (2.11) into (2.9) the equation of motion is

$$\mathbf{M}\ddot{\mathbf{v}} + \mathbf{C}\dot{\mathbf{v}} + \mathbf{K}\mathbf{v} = -\mathbf{M}\mathbf{I}_2\ddot{\mathbf{u}}^{(0)}(t) + \mathbf{I}_1\mathbf{F}(t) \quad , \quad t > 0$$

$$\mathbf{v}(0) = -\mathbf{I}_2\mathbf{u}^{(0)}(0) \; , \; \dot{\mathbf{v}}(0) = -\mathbf{I}_2\dot{\mathbf{u}}^{(0)}(0) \tag{2.12}$$

2.2 Optimal Control of a Discretized System

The equation of motion (2.12) of a discrete-parameter structure under earthquake excitation, $\ddot{\mathbf{u}}^{(0)}(t)$, and active control forces, $\mathbf{F}(t)$, can be described in state space representation as

$$\dot{\mathbf{Y}}(t) = \mathbf{A}(t)\mathbf{Y}(t) + \mathbf{B}_1\ddot{\mathbf{u}}^{(0)}(t) + \mathbf{B}_2\mathbf{F}(t)$$

$$\mathbf{Y}(t_0) = \mathbf{Y}_0 \tag{2.13}$$

where

$$\mathbf{Y}(t) = \begin{bmatrix} \mathbf{v}(t) \\ \dot{\mathbf{v}}(t) \end{bmatrix} \quad, \quad \mathbf{Y}_0 = \begin{bmatrix} -\mathbf{I}_2\mathbf{u}^{(0)}(0) \\ -\mathbf{I}_2\dot{\mathbf{u}}^{(0)}(0) \end{bmatrix} \tag{2.14}$$

$$\mathbf{A} = \begin{bmatrix} \mathbf{0} & \mathbf{E} \\ -\mathbf{M}^{-1}\mathbf{K} & -\mathbf{M}^{-1}\mathbf{C} \end{bmatrix} \quad, \quad \mathbf{B}_1 = \begin{bmatrix} \mathbf{0} \\ -\mathbf{I}_2 \end{bmatrix} \quad, \quad \mathbf{B}_2 = \begin{bmatrix} \mathbf{0} \\ \mathbf{M}^{-1}\mathbf{I}_1 \end{bmatrix} \tag{2.15}$$

$\ddot{\mathbf{u}}^{(0)}(t)$ is assumed to be the real earthquake accelerations in the degrees of freedom at the base, for instance in the form of a measured or a simulated earthquake signal.

If $\ddot{\mathbf{u}}^{(0)}(t)$ is not known a priori and has random characters, it is natural to use a stochastic model. Here, $\ddot{\mathbf{u}}^{(0)}(t)$ is then interpreted as the derivative process with respect to time $\{\dot{\mathbf{W}}(t), t \in [0,\infty[\}$ of a Wiener process $\{\mathbf{W}(t), t \in [0,\infty[\}$. A Wiener process is a Gaussian process for which $\mathbf{W}(t) = \mathbf{0}$ with probability 1, and for which the component processes $\{ W_i(t) , t \in [0,\infty[, i = 1,2,....,m \}$, obey the incremental properties

$$E[\mathrm{d}W_i(t)] = 0 \tag{2.16}$$

$$E[\mathrm{d}W_i(t_1)\mathrm{d}W_j(t_2)] = \begin{cases} 0 , & i \neq j \ \bigvee \ t_1 \neq t_2 \\ \mathrm{d}t , & i = j \ \bigwedge \ t_1 = t_2 \end{cases} \tag{2.17}$$

Hence, $\{\dot{\mathbf{W}}(t), t \in [0,\infty[\}$ may be interpreted as a white Gaussian noise.

A more realistic stochastic model for the earthquake acceleration may be obtained by describing $\ddot{\mathbf{u}}^{(0)}(t)$ as a filtered white noise process. If so the integrated system made up of the equation of motion and the filter equation, given by an ordinary, linear differential equation, can still be written in state space form as (2.13).

The optimal control system is designed in such a way that the vibration of the structure is minimized, using "acceptable" levels of control forces. The level of the vibration and the control forces is formulated mathematically by a so called *performance index* or *loss function*.

If $\ddot{\mathbf{u}}^{(0)}(t)$ is deterministic the classical quadratic performance index is written as

$$\begin{aligned} J &= J(\{\mathbf{F}(t), \ t \in [t_0, T[\}, \mathbf{Y}(t_0), t_0) \\ &= \frac{1}{2}\mathbf{Y}^T(T)\mathbf{S}(T)\mathbf{Y}(T) + \frac{1}{2}\int_{t_0}^T \left(\mathbf{Y}^T(t)\mathbf{Q}(t)\mathbf{Y}(t) + \mathbf{F}^T(t)\mathbf{R}(t)\mathbf{F}(t)\right)\mathrm{d}t \end{aligned} \tag{2.18}$$

$\mathbf{S}(T)$ and $\mathbf{Q}(t)$ are positive semidefinite symmetric weighting matrices and $\mathbf{R}(t)$ is a positive definite symmetric weighting matrix. The time interval $[t_0, T[$ is the period of the ground motion excitation, i.e., for $t \geq T$, $\ddot{\mathbf{u}}^{(0)}(t) = \mathbf{0}$. The specification of the performance index $J = J(\{\mathbf{F}(t), \ t \in [t_0, T[\}, \mathbf{Y}(t_0), t_0)$ indicates that J is a functional of $\mathbf{F}(t)$, and a function of the initial conditions $\mathbf{Y}(t_0)$ and the starting time t_0.

If $\{\ddot{\mathbf{u}}_0(t), t \in [t_0, T[\}$ is a stochastic process, the expected value of the right hand side of (2.18) is used.

2.2.1   Determination of the Control Forces

The optimal control $\{\mathbf{F}^*(t),\ t \in [t_0, T[\}$ is obtained as the loading history minimizing (2.18). The minimum value of the functional (2.18) is

$$
\begin{aligned}
J^* \;=\; J^*(\mathbf{Y}(t_0), t_0) =\; & \min_{\{\mathbf{F}(t),\, t\, \in\, [t_0,\, T[\}} \left(\frac{1}{2}\mathbf{Y}^T(T)\mathbf{S}(T)\mathbf{Y}(T) \right. \\
& \left. + \frac{1}{2}\int_{t_0}^{T} \left(\mathbf{Y}^T(t)\mathbf{Q}(t)\mathbf{Y}(t) + \mathbf{F}^T(t)\mathbf{R}(t)\mathbf{F}(t) \right)\mathrm{d}t \right)
\end{aligned}
\tag{2.19}
$$

In addition the optimally controlled state $\mathbf{Y}^*(t)$, caused by the optimal control force $\mathbf{F}^*(t)$, is going to be determined.

In eq. (2.18) t_0 is considered as a variable.

The problem of finding the optimal function $J^*(\mathbf{Y}(t), t)$ can be converted into a problem of finding the solution to a system of partial differential equations. The theory for deriving these equations is based on a generalization of the Hamilton-Jacobi theory. From this theory, called dynamic programming, the following parabolic partial differential equation is derived, ref. [17].

$$
\begin{aligned}
-\frac{\partial J^*}{\partial t} \;=\; & \min_{\mathbf{F}(t)} \left(\frac{1}{2}\mathbf{y}^T\mathbf{Q}(t)\mathbf{y} + \frac{1}{2}\mathbf{F}^T(t)\mathbf{R}(t)\mathbf{F}(t) \right. \\
& \left. + \left(\frac{\partial J^*}{\partial \mathbf{y}}\right)^T \left(\mathbf{A}(t)\mathbf{y} + \mathbf{B}_1\ddot{\mathbf{u}}^{(0)}(t) + \mathbf{B}_2\mathbf{F}(t) \right) \right)
\end{aligned}
\tag{2.20}
$$

This partial differential equation for $J^*(\mathbf{y}, t)$ is called the Hamilton-Jacobi-Bellman equation, (HJB).

Minimum of the right hand side of (2.20) is obtained, when the partial derivative with respect to $\mathbf{F}(t)$ is equal $\mathbf{0}$. This leads to the condition

$$
\mathbf{R}(t)\mathbf{F}^*(t) + \mathbf{B}_2^T\frac{\partial J^*}{\partial \mathbf{y}} = \mathbf{0}
\tag{2.21}
$$

In the derivation of (2.21) it is used that $\mathbf{R}(t)$ is symmetric. Rearranging (2.21) the optimal control force $\mathbf{F}^*$ is seen to be

$$
\mathbf{F}^*(t) = -\mathbf{R}^{-1}(t)\mathbf{B}_2^T\frac{\partial J^*}{\partial \mathbf{y}}
\tag{2.22}
$$

Substituting (2.22) into (2.20) we have

$$
\begin{aligned}
-\frac{\partial J^*}{\partial t} \;=\; & \frac{1}{2}\mathbf{y}^T\mathbf{Q}(t)\mathbf{y} - \frac{1}{2}\left(\frac{\partial J^*}{\partial \mathbf{y}}\right)^T \mathbf{B}_2\mathbf{R}^{-1}(t)\mathbf{B}_2^T\left(\frac{\partial J^*}{\partial \mathbf{y}}\right) \\
& + \left(\frac{\partial J^*}{\partial \mathbf{y}}\right)^T \mathbf{A}(t)\mathbf{y} + \left(\frac{\partial J^*}{\partial \mathbf{y}}\right)^T \mathbf{B}_1\ddot{\mathbf{u}}^{(0)}(t)
\end{aligned}
\tag{2.23}
$$

The final condition to the partial differential equation (2.23) is found by setting $t_0 = T$ in (2.18)

$$
J^*(\mathbf{y}, T) = \frac{1}{2}\mathbf{y}^T\mathbf{S}_T\mathbf{y} \ , \quad \mathbf{S}_T = \mathbf{S}(T)
\tag{2.24}
$$

which is to be fulfilled for all values of $\mathbf{y}$.

Eq. (2.23) is solved by assuming a solution given by

$$J^*(\mathbf{y}, t) = \frac{1}{2}\mathbf{y}^T \mathbf{S}(t)\mathbf{y} + \mathbf{T}^T(t)\mathbf{y} + V(t), \tag{2.25}$$

where $\mathbf{S}(t)$ is an unknown symmetric matrix, $\mathbf{T}(t)$ is an unknown vector and $V(t)$ is an unknown scalar. The necessary condition that the assumed solution exists is found by substituting (2.25) into (2.23),

$$\frac{1}{2}\mathbf{y}^T\left(\dot{\mathbf{S}}(t) + \mathbf{S}(t)\mathbf{A}(t) + \mathbf{A}^T(t)\mathbf{S}(t) - \mathbf{S}(t)\mathbf{B}_2\mathbf{R}^{-1}(t)\mathbf{B}_2^T\mathbf{S}(t) + \mathbf{Q}(t)\right)\mathbf{y}$$
$$+ \mathbf{y}^T\left(\mathbf{A}^T(t)\mathbf{T}(t) + \dot{\mathbf{T}}(t) - \mathbf{S}(t)\mathbf{B}_2\mathbf{R}^{-1}(t)\mathbf{B}_2^T\mathbf{T}(t) + \mathbf{S}(t)\mathbf{B}_1\ddot{\mathbf{u}}^{(0)}(t)\right)$$
$$+ \mathbf{T}^T(t)\mathbf{B}_1\ddot{\mathbf{u}}^{(0)}(t) + \dot{V}(t) - \frac{1}{2}\mathbf{T}^T(t)\mathbf{B}_2\mathbf{R}^{-1}(t)\mathbf{B}_2^T\mathbf{T}(t) = 0 \tag{2.26}$$

Since (2.26) holds for all states $\mathbf{y}$, we require that the quadratic term in $\mathbf{y}$, the linear term, and the terms not involving $\mathbf{y}$ must balance individually. Therefore,

$$\dot{\mathbf{S}} + \mathbf{S}(t)\mathbf{A}(t) + \mathbf{A}^T(t)\mathbf{S}(t) - \mathbf{S}(t)\mathbf{B}_2\mathbf{R}^{-1}(t)\mathbf{B}_2^T\mathbf{S}(t) + \mathbf{Q}(t) = \mathbf{0} \tag{2.27}$$

$$\dot{\mathbf{T}}(t) + \mathbf{A}^T(t)\mathbf{T}(t) - \mathbf{S}(t)\mathbf{B}_2\mathbf{R}^{-1}(t)\mathbf{B}_2^T\mathbf{T}(t) + \mathbf{S}(t)\mathbf{B}_1\ddot{\mathbf{u}}^{(0)}(t) = \mathbf{0} \tag{2.28}$$

$$\dot{V}(t) + \mathbf{T}^T(t)\mathbf{B}_1\ddot{\mathbf{u}}^{(0)}(t) - \frac{1}{2}\mathbf{T}^T(t)\mathbf{B}_2\mathbf{R}^{-1}(t)\mathbf{B}_2^T\mathbf{T}(t) = 0 \tag{2.29}$$

(2.27) is a matrix *Ricatti equation*.

Using the assumption $\ddot{\mathbf{u}}^{(0)}(T) = \mathbf{0}$, (2.24) and (2.25) result in the following final conditions for $\mathbf{S}(t)$, $\mathbf{T}(t)$ and $V(t)$

$$\mathbf{S}(T) = \mathbf{S}_T$$

$$\mathbf{T}(T) = \mathbf{0}$$

$$V(T) = 0 \tag{2.30}$$

The condition $\ddot{\mathbf{u}}^{(0)}(T) = \mathbf{0}$ provides that (2.28) fulfils (2.30) for $t = T$.

The partial derivative of (2.25) with respect to $\mathbf{y}$ is given by

$$\frac{\partial J^*}{\partial \mathbf{y}} = \mathbf{S}(t)\mathbf{y} + \mathbf{T}(t) \tag{2.31}$$

The optimal control force then follows by inserting (2.31) into (2.22),

$$\mathbf{F}^*(t) = -\mathbf{R}^{-1}(t)\mathbf{B}_2^T\mathbf{S}(t)\mathbf{Y}(t) - \mathbf{R}^{-1}(t)\mathbf{B}_2^T\mathbf{T}(t) \tag{2.32}$$

The first term in (2.32) represents the *closed-loop* control, i.e. the term depending on the current state $\mathbf{Y}(t)$. The second term represents the *open-loop* control, which is independent of the vibration of the structure, but it depends on the external loading through $\mathbf{T}$. The closed-loop control force is designated $\mathbf{F}^{(c)}(t)$, whereas the open-loop control force is designated $\mathbf{F}^{(o)}(t)$. Thus, eq. (2.32) is written in the form

$$\mathbf{F}^*(t) = \mathbf{F}^{(c)}(t) + \mathbf{F}^{(o)}(t) \tag{2.33}$$

Using closed-loop control and open-loop control, respectively, the response is designated $\mathbf{Y}^{(c)}(t)$ and $\mathbf{Y}^{(o)}(t)$.

Closed-loop control is only optimal if $\mathbf{T}(t) \equiv \mathbf{0}$. Hence, it follows from (2.28) and the final condition $\mathbf{T}(t) = \mathbf{0}$ that $\ddot{\mathbf{u}}^{(0)}(t) = \mathbf{0}, t \in [t_0, T[$ has to be valid, corresponding an autonomous system of the structure and controllers.

In what follows closed-loop control is also used to control structures subjected to external loading. This is an applicable control device, when the first term on the right hand side of (2.32) is dominating in relation to the last term. However, if the motion is relatively small, measured by any norm of $\mathbf{Y}(t)$, it is not valid. In this case open-loop control ought to be employed. Using closed-loop control, the control system becomes instable when the motion is damped out. This phenomenon appears from an example in chapter 4.

A feedback gain $\mathbf{G}(t)$ is defined as

$$\mathbf{G}(t) = \mathbf{R}^{-1}(t)\mathbf{B}_2^T\mathbf{S}(t) \tag{2.34}$$

Then for the case of closed-loop control one has

$$\mathbf{F}^{(c)}(t) = -\mathbf{G}(t)\mathbf{Y}^{(c)}(t) \tag{2.35}$$

Applying closed-loop control the motion can be obtained by substituting (2.35) into (2.13)

$$\dot{\mathbf{Y}}^{(c)}(t) = \left(\mathbf{A}(t) - \mathbf{B}_2\mathbf{G}(t) \right) \mathbf{Y}^{(c)}(t) + \mathbf{B}_1\ddot{\mathbf{u}}^{(0)}(t), \quad \mathbf{Y}^{(c)}(t_0) = \mathbf{Y}_0 \tag{2.36}$$

Under closed-loop control the motion $\mathbf{Y}^{(c)}(t)$ is obtained by solving (2.36) numerically given the initial state $\mathbf{Y}_0$. This procedure is used by numerical simulations of the control system. In practice $\mathbf{Y}^{(c)}(t)$ is measured and inserted directly into (2.35) to obtain the closed-loop control force.

In order to determine the cost, $J(\mathbf{Y}(t_0), t_0)$ of controlling the structure in the interval $[t_0, T[$ the following identity is used

$$\mathbf{Y}^T(T)\mathbf{S}(T)\mathbf{Y}(T) - \mathbf{Y}^T(t_0)\mathbf{S}(t_0)\mathbf{Y}(t_0)$$
$$= \int_{t_0}^T \frac{\mathrm{d}}{\mathrm{d}t} \left(\mathbf{Y}^T(t)\mathbf{S}(t)\mathbf{Y}(t) \right) \mathrm{d}t$$
$$= \int_{t_0}^T \left(\left(\mathbf{A}(t)\mathbf{Y}(t) + \mathbf{B}_1\ddot{\mathbf{u}}^{(0)}(t) + \mathbf{B}_2\mathbf{F}(t) \right)^T \mathbf{S}(t)\mathbf{Y}(t) + \mathbf{Y}^T(t)\dot{\mathbf{S}}(t)\mathbf{Y}(t) \right.$$
$$\left. + \mathbf{Y}^T(t)\mathbf{S}(t) \left(\mathbf{A}(t)\mathbf{Y}(t) + \mathbf{B}_1\ddot{\mathbf{u}}^{(0)}(t) + \mathbf{B}_2\mathbf{F}(t) \right) \right) \mathrm{d}t \tag{2.37}$$

In the context of closed-loop control the cost is obtained by substituting (2.27), (2.34), (2.35) and (2.37) into (2.18). After rearranging, this yields

$$J^{(c)}(\mathbf{Y}^{(c)}(t_0), t_0) = \frac{1}{2}\mathbf{Y}^{(c)T}(t_0)\mathbf{S}(t_0)\mathbf{Y}^{(c)}(t_0) + \frac{1}{2}\int_{t_0}^T \left(\ddot{\mathbf{u}}_0^T(t)\mathbf{B}_1^T\mathbf{S}(t)\mathbf{Y}^{(c)}(t) \right.$$
$$\left. + \mathbf{Y}^{(c)T}(t)\mathbf{S}(t)\mathbf{B}_1\ddot{\mathbf{u}}_0(t) \right) \mathrm{d}t \tag{2.38}$$

Let $\ddot{\mathbf{u}}^{(0)}(t)$ be a white noise process and equation (2.13) be an Itô-differential equation. The increment $\mathrm{d}\mathbf{W}(t) = \mathbf{W}(t + \mathrm{d}t) - \mathbf{W}(t)$ of the Wiener process and $\mathbf{Y}^{(c)}(t)$ then becomes stochastically independent, since $\mathbf{Y}^{(c)}(t)$ only depends on the stochastic variables $\{\mathbf{W}(\tau), \ \tau \in [t_0, t[\}$. Hence it follows that $\mathrm{E}[\mathrm{d}\mathbf{W}^T(t)\mathbf{B}_1\mathbf{S}(t)\mathbf{Y}^{(c)}(t)] = \mathrm{E}[\mathrm{d}\mathbf{W}^T(t)]\mathbf{B}_1\mathbf{S}(t)\mathrm{E}[\mathbf{Y}^{(c)}(t)] = 0$. Performing the expectation on both sides of (2.38), the

stochastic integral then vanishes. Consequently, the loss function in case of white noise processes yields

$$\mathrm{E}\left[J^{(c)}(\mathbf{Y}(t_0), t_0)\right] = \frac{1}{2}\mathbf{Y}^T(t_0)\mathbf{S}(t_0)\mathbf{Y}(t_0) \tag{2.39}$$

In (2.39) it is assumed that the initial condition $\mathbf{Y}^{(c)}(t_0) = \mathbf{Y}_0$ is deterministic.

2.2.2 The Steady-State Solution to the Ricatti Equation

In what follows a constant feedback gain $\mathbf{G}$ will be proposed for application to a constant system matrix $\mathbf{A}$ and weighting matrices $\mathbf{Q}$, $\mathbf{R}$.

The solution, $\mathbf{S}(t)$, to the Ricatti equation (2.27) may under certain conditions converge to a limiting symmetric matrix $\mathbf{S}(\infty)$, when $(T - t) \rightarrow \infty$. If so, the corresponding steady-state feedback gain, $\mathbf{G}$, can be written

$$\mathbf{G}(\infty) = \mathbf{R}^{-1}\mathbf{B}_2^T\mathbf{S}(\infty) \tag{2.40}$$

Applying the limiting feedback gain, $\mathbf{G}(\infty)$, as well in the transient phase, the closed-loop control law then is

$$\mathbf{F}^{(c)}(t) = -\mathbf{G}(\infty)\mathbf{Y}^{(c)}(t) \tag{2.41}$$

If $\mathbf{S}(t)$ does converge, then $\lim_{(T-t) \rightarrow \infty} \dot{\mathbf{S}} = \mathbf{0}$, which in the limit results in a quadratic equation, cf. (2.28).

$$\mathbf{A}^T\mathbf{S} + \mathbf{S}\mathbf{A} - \mathbf{S}\mathbf{B}_2\mathbf{R}^{-1}\mathbf{B}_2^T\mathbf{S} + \mathbf{Q} = \mathbf{0}, \tag{2.42}$$

Generally, more than one solution exist to (2.42), called a *Lyapunov* equation. Each solution is obtained with different initial conditions $\mathbf{S}(t_0)$ to (2.27). Indeed, the solution space $R^{n \times n}$ is split up into disjoint subspaces, where every initial condition $\mathbf{S}(t_0) \in R^{n \times n}$ belonging to the same subspace, leads to a solution $\mathbf{S}(t)$, which is attracted to one and the same solution to (2.42).

Some of the solutions to (2.42) may be eliminated by requiring that $\mathbf{S}$ is positive definite, [17].

On the assumption that a system is controlled considerably longer than the duration of the external loading, we have $\mathbf{Y}^{(c)}(T) = \mathbf{0}$. Hence, it follows that (2.63) is the control law for the infinite horizon performance index

$$J^{(c)}(\infty) = \frac{1}{2}\int_{t_0}^{\infty}\left(\mathbf{Y}^{(c)T}(t)\mathbf{Q}\mathbf{Y}^{(c)}(t) + \mathbf{F}^{(c)T}(t)\mathbf{R}\mathbf{F}^{(c)}(t)\right)\mathrm{d}t \tag{2.43}$$

According to [9], the efficiency of a control system is not affected, when the Ricatti matrix is approximated by the steady-state matrix, as long as the control period is longer than the earthquake duration. In [9] this conclusion is based on investigations concerning an eight storey building under earthquake excitation.

2.3 Independent Modal Space Control

In this section the device of independent modal space control is presented. The basis is the distributed parameter system described in section 2.1.

Consider the associated homogeneous kinematical boundary conditions of (2.3),

$$u_i(\mathbf{x}, t) = 0 \quad, \quad \forall\, (\mathbf{x}, t) \in \Gamma_2 \times\,]0, \infty[\tag{2.44}$$

Since $U_i^{(0)}(\mathbf{x},t)$ fulfils the nonhomogeneous boundary conditions (2.7), it follows that $u_i(\mathbf{x},t)$ - $U_i^{(0)}(\mathbf{x},t)$ fulfils the homogeneous boundary conditions (2.2) and (2.44). Consequently, the solution to (2.1)-(2.4) can be given in the form

$$u_i(\mathbf{x},t) \;=\; U_i^{(0)}(\mathbf{x},t) \;+\; \sum_{m=1}^{\infty} \Phi_i^{(m)}(\mathbf{x})q_m(t) \tag{2.45}$$

where $\Phi_i^{(m)}$ are the linear eigenmodes and $q_m(t)$ are the modal coordinates. $\Phi_i^{(m)}$ are obtained from the linear eigenvalue problem

$$L\Phi_i^{(m)}(\mathbf{x}) \;-\; \omega_m^2\rho(\mathbf{x})\Phi_i^{(m)}(\mathbf{x}) \;=\; 0 \quad , \quad \forall\,\mathbf{x}\in\Omega \quad , \quad m \;=\; 1,2,.... \tag{2.46}$$

$$B_1\Phi_i^{(m)} \;=\; 0 \quad , \quad \forall\,\mathbf{x}\in\Gamma_1 \quad , \quad m \;=\; 1,2,.... \tag{2.47}$$

$$\Phi_i^{(m)} \;=\; 0 \quad , \quad \forall\,\mathbf{x}\in\Gamma_2 \quad , \quad m \;=\; 1,2,.... \tag{2.48}$$

ω_1^2, ω_2^2, ... are the cyclical eigenfrequencies. Assuming L is self-adjoint and positive definite, all cyclical eigenfrequencies are real and positive. Further, the eigenfunctions fulfil the following orthogonality properties

$$\int_\Omega \rho(\mathbf{x})\Phi_i^{(m)}(\mathbf{x})\Phi_i^{(n)}(\mathbf{x})\,\mathrm{d}V \;=\; \begin{cases} 0, & m \neq n \\ M_m, & m = n \end{cases} \tag{2.49}$$

$$\int_\Omega \Phi_i^{(m)}(\mathbf{x})L\Phi_i^{(n)}(\mathbf{x})\,\mathrm{d}V \;=\; \begin{cases} 0, & m \neq n \\ \omega_m^2 M_m, & m = n \end{cases} \tag{2.50}$$

M_m signifies the modal mass defined as

$$M_m \;=\; \int_\Omega \rho(\mathbf{x})\Phi_i^{(m)}(\mathbf{x})\Phi_i^{(m)}(\mathbf{x})\,\mathrm{d}V \quad , \quad m \;=\; 1,2,.... \tag{2.51}$$

Introducing (2.45) and (2.8) into (2.1), and employing the orthogonality properties (2.49) and (2.50), we obtain

$$\ddot{q}_m \;+\; 2\omega_m\left(\zeta_m\dot{q}_m \;+\; \sum_{n=1,n\neq m}^{\infty}\sqrt{\frac{\omega_n M_n}{\omega_m M_m}}\zeta_{mn}\dot{q}_n\right) \;+\; \omega_m^2 q_m$$
$$=\; a_m(t) \;+\; p_m(t) \quad , \quad m \;=\; 1,2,.... \;, \quad t\,\in\,]0,\infty[\tag{2.52}$$

where the modal external loadings caused by the displacements at the bound Γ_2 are given by

$$a_m(t) \;=\; -\frac{1}{M_m}\int_\Omega \Phi_i^{(m)}(\mathbf{x})\rho(\mathbf{x})\frac{\partial^2}{\partial t^2}U_i^{(0)}(\mathbf{x},t)\,\mathrm{d}V \quad , \quad m \;=\; 1,2,.... \tag{2.53}$$

and the modal control forces can be written as

$$p_m(t) \;=\; \frac{1}{M_m}\mathbf{b}_m^T\mathbf{F}(t) \quad , \quad m \;=\; 1,2,.... \tag{2.54}$$

$$\mathbf{b}_m \;=\; \begin{bmatrix} \Phi_i^{(m)}(\mathbf{x}_1)e_{1i} \\ \Phi_i^{(m)}(\mathbf{x}_2)e_{2i} \\ \cdot \\ \cdot \\ \cdot \\ \cdot \\ \Phi_i^{(m)}(\mathbf{x}_{n_m})e_{m_n i} \end{bmatrix} \qquad \mathbf{F}(t) \;=\; \begin{bmatrix} F_1(t) \\ F_2(t) \\ \cdot \\ \cdot \\ \cdot \\ \cdot \\ F_{n_m}(t) \end{bmatrix} \tag{2.55}$$

The damping ratio ζ_m in the mth mode is defined as

$$\zeta_m = \frac{\sum_{i=1}^{3}\int_{\Omega}c(\mathbf{x})\Phi_i^{(m)}(\mathbf{x})\Phi_i^{(m)}(\mathbf{x})\,\mathrm{d}V}{2\omega_m M_m} \tag{2.56}$$

The coefficients ζ_{mn} determine a coupling in the system caused by linear viscous structural damping. They are given by

$$\zeta_{mn} = \frac{\sum_{i=1}^{3}\int_{\Omega}c(\mathbf{x})\Phi_i^{(m)}(\mathbf{x})\Phi_i^{(n)}(\mathbf{x})\,\mathrm{d}V}{2\sqrt{\omega_m\omega_n M_m M_n}} \tag{2.57}$$

In the absence of feedback control forces (2.52) represents a coupled system of differential equations. This coupling is referred to as *internal*. If feedback control forces are present, however, and the modal feedback control forces $p_m(t)$ depend on all modal coordinates $q_1, q_2, \dots$ and their velocities $\dot{q}_1, \dot{q}_2, \dots$, i.e.

$$p_m(t) = p_m(q_1, q_2, \dots ;\ \dot{q}_1, \dot{q}_2, \dots) \tag{2.58}$$

then equations (2.52) are *externally* coupled.

According to (2.57) a necessary and sufficient condition for internal decoupling is

$$\sum_{i=1}^{3}\int_{\Omega}c(\mathbf{x})\Phi_i^{(m)}(\mathbf{x})\Phi_i^{(n)}(\mathbf{x})\,\mathrm{d}V = 0 \quad,\quad \forall\, m,n = 1,2,\dots,\ m \neq n \tag{2.59}$$

A sufficient condition for (2.59) is, that $c(\mathbf{x})$ is proportional with $\rho(\mathbf{x})$, cf. (2.49).

In the special case of external decoupling the modal control force in the mth mode $p_m(t)$ only depends on q_m and $\dot{q}_m$, i.e.

$$p_m(t) = p_m(q_m, \dot{q}_m) \quad,\quad m = 1,2,\dots \tag{2.60}$$

(2.59) and (2.60) imply that the control system can be designed for each mode separately, where the design takes place in modal space. This is the essence of the *independent modal space control*.

Assuming eqs. (2.52) are both internally and externally decoupled, we have an infinite set of decoupled second order differential equations

$$\ddot{q}_m + 2\omega_m\zeta_m\dot{q}_m + \omega_m^2 q_m = a_m(t) + p_m(q_m, \dot{q}_m),\ m = 1,2,..,t\in]0,\infty[\tag{2.61}$$

The equation of motion in the mth mode can be written in state form as

$$\dot{\mathbf{Y}}_m(t) = \mathbf{A}_m\mathbf{Y}_m(t) + \mathbf{B}_m\left((a_m(t) + p_m(\mathbf{Y}_m))\right) \tag{2.62}$$

$$\mathbf{Y}_m = \begin{bmatrix} q_m \\ \dot{q}_m \end{bmatrix},\quad \mathbf{A}_m = \begin{bmatrix} 0 & 1 \\ -\omega_m^2 & -2\zeta_m\omega_m \end{bmatrix},\quad \mathbf{B}_m = \begin{bmatrix} 0 \\ 1 \end{bmatrix} \tag{2.63}$$

2.3.1 Closed-Loop Modal Space Control

Let us consider optimal independent modal space control. In this case the performance index is taken in the form

$$J = \sum_{m=1}^{n_c} J_m \tag{2.64}$$

where J_m is the modal loss function chosen as

$$J_m = M_m \frac{1}{2} \int_{t_0}^{T} \left(\mathbf{Y}_m^T(t) \mathbf{Q}_m \mathbf{Y}_m(t) + r_m p_m^2(t) \right) dt \tag{2.65}$$

n_c is the number of controlled modes. $\mathbf{Q}_m$ is a positive semidefinite weighting matrix of dimension 2×2. r_m is a positive weighting coefficient.

A logical choice for $\mathbf{Q}_m$ is

$$\mathbf{Q}_m = \begin{bmatrix} \omega_m^2 & 0 \\ 0 & 1 \end{bmatrix} \tag{2.66}$$

so that the first term in (2.65) represents the total mechanical energy associated with the mth mode.

Due to the modal decoupling the minimization of the performance index J can be achieved by minimizing each and every modal cost function J_m independently. The minimization of J_m leads to the modal feedback force, cf. (2.35)

$$p_m^{(c)}(t) = -\mathbf{G}_m(t) \mathbf{Y}_m^{(c)}(t) \tag{2.67}$$

$\mathbf{G}_m(t)$ is a 1×2 modal feedback gain matrix given by, cf. (2.42)

$$\mathbf{G}_m(t) = \frac{1}{r_m} \mathbf{B}_m^T \mathbf{S}_m(t) = [g_{1,m}(t) \quad g_{2,m}(t)] \tag{2.68}$$

$$g_{1,m}(t) = \frac{s_{2,m}(t)}{r_m} \tag{2.69}$$

$$g_{2,m}(t) = \frac{s_{3,m}(t)}{r_m} \tag{2.70}$$

where

$$\mathbf{S}_m(t) = \begin{bmatrix} s_{1,m}(t) & s_{2,m}(t) \\ s_{2,m}(t) & s_{3,m}(t) \end{bmatrix} \tag{2.71}$$

The optimal closed-loop modal controls can then be written in the form

$$p_m^{(c)}(t) = -g_{1,m}(t) q_m - g_{2,m}(t) \dot{q}_m \quad , \quad m = 1, 2, ..., n_c \tag{2.72}$$

The associated closed-loop equations are obtained by substituting (2.72) into (2.61),

$$\ddot{q}_m + \left(2\omega_m \zeta_m + g_{2,m}(t) \right) \dot{q}_m + \left(\omega_m^2 + g_{1,m}(t) \right) q_m = a_m(t),$$
$$m = 1, 2, ..., n_c \ t \in]0, \infty[\tag{2.73}$$

2.3.2 The Ricatti Equation by Independent Modal Space Control

The symmetric weighting matrix $\mathbf{S}_m(t)$ satisfies the matrix Ricatti equation, cf. (2.27)

$$\dot{\mathbf{S}}_m + \mathbf{S}_m \mathbf{A}_m(t) + \mathbf{A}_m^T(t) \mathbf{S}_m - \frac{1}{r_m} \mathbf{S}_m \mathbf{B}_m \mathbf{B}_m^T \mathbf{S}_m + \mathbf{Q}_m = \mathbf{0} \tag{2.74}$$

Inserting (2.63), (2.66) and (2.71) into (2.74) results in the following three coupled 1.order differential equations

$$\dot{s}_{1,m}(t) - 2\omega_m^2 s_{2,m}(t) - \frac{1}{r_m} s_{2,m}^2(t) + \omega_m^2 = 0 \tag{2.75}$$

$$\dot{s}_{2,m}(t) + s_{1,m}(t) - 2\zeta_m\omega_m s_{2,m}(t) - \omega_m^2 s_{3,m}(t) - \frac{1}{r_m}s_{2,m}(t)s_{3,m}(t) = 0 \qquad (2.76)$$

$$\dot{s}_{3,m}(t) + 2s_{2,m}(t) - 4\zeta_m\omega_m s_{3,m}(t) - \frac{1}{r_m}s_{3,m}^2(t) + 1 = 0 \qquad (2.77)$$

(2.75)-(2.77) can only be solved numerically. The steady-state solution, however, is easy to obtain. Letting $\dot{s}_{1,m}(t) = \dot{s}_{2,m}(t) = \dot{s}_{3,m}(t) = 0$, three nonlinear algebraic equations are obtained. These can be solved to give

$$s_{1,m} = 2\zeta_m\omega_m s_{2,m} + \omega_m^2 s_{3,m} + \frac{s_{2,m}s_{3,m}}{r_m}$$

$$s_{2,m} = \omega_m^2 r_m \left(\pm\sqrt{1 + \frac{1}{\omega_m^2 r_m}} - 1 \right) \qquad (2.78)$$

$$s_{3,m} = 2\zeta_m\omega_m r_m \left(\pm\sqrt{1 + \frac{1 + 2s_{2,m}}{4\zeta_m^2\omega_m^2 r_m}} - 1 \right)$$

In order that $\mathbf{S}_m$ can be positive semi-definite it is required that $s_{1,m} > 0$, $s_{3,m} > 0$, and $s_{1,m}s_{3,m} > s_{2,m}^2$. By this the negative solutions in (2.78) may be eliminated for $s_{2,m}$ and $s_{3,m}$, leading to

$$s_{1,m} = 2\zeta_m\omega_m s_{2,m} + \omega_m^2 s_{3,m} + \frac{s_{2,m}s_{3,m}}{r_m}$$

$$s_{2,m} = \omega_m^2 r_m \left(\sqrt{1 + \frac{1}{\omega_m^2 r_m}} - 1 \right) \qquad (2.79)$$

$$s_{3,m} = 2\zeta_m\omega_m r_m \left(\sqrt{1 + \frac{1 + 2s_{2,m}}{4\zeta_m^2\omega_m^2 r_m}} - 1 \right)$$

Finally, the steady-state feedback gains $g_{1,m}$ and $g_{2,m}$ are obtained by inserting (2.79) into (2.69) and (2.70), respectively. The modal controls are then determined.

2.3.3 Spillover

In practice implementation of the independent modal space control scheme described above induces control and observation spillover problems. These phenomena are explained in this section.

The modal control forces $p_m(t)$ determined from (2.72) are only abstract forces. The actual control forces are synthesized from the modal control forces by solving (2.54). These equations only have a unique solution provided the number of actuators n_m is equal to the number of controlled modes, n_c. Further, equations (2.54) imply that the actual control forces $\mathbf{F}(t)$, excite every single mode. Of course, these forces are selected so that the vibratory motion of the controlled modes is suppressed. In the process, the uncontrolled modes are also excited, the phenomenon that has come to be known as *control spillover*.

The importance of control spillover may not be too great, if the number of controlled modes is large. This is due to the placement and regulation of the controllers, whose spatial locations are generally chosen so as to optimize their effect on the controlled

modes. Hence, they tend to act in a "random" fashion on the uncontrolled modes and cancel each other's effect. For the same reason most of the energy in the frequency spectrum for the controllers is concentrated about the eigenfrequencies of the controlled modes. Hence, the effect of control spillover is less, the more the eigenfrequencies of controlled and uncontrolled modes differs. Evidently, two modes with closely related eigenfrequencies both have to be controlled, or both left uncontrolled.

Consider the energy level of the mth mode given as

$$E_m = \frac{1}{2} \left(\dot{q}_m^2 + q_m^2 \omega_m^2 \right) M_m \tag{2.80}$$

(2.80) can be used to reduce the effect of control spillover. If the modal energy in some of the uncontrolled modes exceeds that of the controlled modes, the actuators are switched to control these high energy modes in order to damp their vibration.

In what follows the phenomenon of observation spillover is explained.

$\mathbf{Z}^T(t) = [Z_1(t), ..., Z_{n_c}(t)]$ is assumed to be an n_c-dimensional vector of discrete measurements. $Z_\alpha(t)$ determines the displacement of the point with the reference coordinates $\mathbf{x}_\alpha^T = [x_{\alpha 1}, x_{\alpha 2}, x_{\alpha 3}]$ in a direction given by the unit vector $\mathbf{e}_\alpha^T = [e_{\alpha 1}, e_{\alpha 2}, e_{\alpha 3}]$. The displacement field $\mathbf{u}(\mathbf{x}, t)$ is given by (2.45). By this,

$$Z_\alpha(t) = \mathbf{e}_\alpha^T \mathbf{U}^{(0)}(\mathbf{x}_\alpha, t) + \sum_{m=1}^{\infty} \mathbf{e}_\alpha^T \mathbf{\Phi}^{(m)}(\mathbf{x}_\alpha) q_m(t) \ , \ \alpha = 1, ..., n_c \tag{2.81}$$

If only n_c modes are controlled, one obtains

$$\begin{bmatrix} Z_1 \\ \cdot \\ \cdot \\ Z_{n_c} \end{bmatrix} = \begin{bmatrix} \mathbf{e}_1^T \mathbf{U}^{(0)}(\mathbf{x}_1, t) \\ \cdot \\ \cdot \\ \mathbf{e}_{n_c}^T \mathbf{U}^{(0)}(\mathbf{x}_{n_c}, t) \end{bmatrix} + \begin{bmatrix} D_{11} & \cdot & \cdot & D_{1n_c} \\ \cdot & & & \cdot \\ \cdot & & & \cdot \\ D_{n_c 1} & \cdot & \cdot & D_{n_c n_c} \end{bmatrix} \begin{bmatrix} q_1 \\ \cdot \\ \cdot \\ q_{n_c} \end{bmatrix} \iff$$

$$\begin{bmatrix} q_1 \\ \cdot \\ \cdot \\ q_{n_c} \end{bmatrix} = \mathbf{D}^{-1} \left(\begin{bmatrix} Z_1 \\ \cdot \\ \cdot \\ Z_{n_c} \end{bmatrix} - \begin{bmatrix} \mathbf{e}_1^T \mathbf{U}^{(0)}(\mathbf{x}_1, t) \\ \cdot \\ \cdot \\ \mathbf{e}_{n_c}^T \mathbf{U}^{(0)}(\mathbf{x}_{n_c}, t) \end{bmatrix} \right) \tag{2.82}$$

where the components in $\mathbf{D}$ are given by

$$D_{ij} = \mathbf{e}_i^T \mathbf{\Phi}^{(j)}(\mathbf{x}_i) \tag{2.83}$$

It is seen from (2.83) that the time derivatives of the modal coordinates are

$$\begin{bmatrix} \dot{q}_1 \\ \cdot \\ \cdot \\ \dot{q}_{n_c} \end{bmatrix} = \mathbf{D}^{-1} \left(\begin{bmatrix} \dot{Z}_1 \\ \cdot \\ \cdot \\ \dot{Z}_{n_c} \end{bmatrix} - \begin{bmatrix} \mathbf{e}_1^T \dot{\mathbf{U}}^{(0)}(\mathbf{x}_1, t) \\ \cdot \\ \cdot \\ \mathbf{e}_{n_c}^T \dot{\mathbf{U}}^{(0)}(\mathbf{x}_{n_c}, t) \end{bmatrix} \right) \tag{2.84}$$

By the experiments the accelerations $\ddot{\mathbf{Z}}(t)$ are measured. $\mathbf{Z}(t)$ and $\dot{\mathbf{Z}}(t)$ are then obtained by numerical integration of the acceleration signals. Next, the components $(q_m, \dot{q}_m)$, $m = 1, ..., n_c$, contained in the modal control law (2.67) are determined from (2.82) and (2.84).

The *observable spillover* $\Delta Z_\alpha(t)$ is the difference between the real displacements (2.81) and those determined from the "truncated" measurements (2.82) and (2.83)

$$\Delta Z_\alpha(t) = Z_\alpha(t) - \mathbf{e}_\alpha^T \mathbf{U}^{(0)}(\mathbf{x}_\alpha, t) - \sum_{m=1}^{n_c} \mathbf{e}_\alpha^T \mathbf{\Phi}^{(m)}(\mathbf{x}_\alpha) q_m(t), \alpha = 1, .., n_c \tag{2.85}$$

Eqs. (2.85) contain modal coordinates calculated from (2.82). Truncating the series (2.81) they will always be an approximation of the exact modal coordinates in (2.81). When the control forces are determined on the basis of (2.82) and (2.83) an inferior control is obtained than if the correct modal coordinates had been used. Hence, the observation spillover expresses the error caused by truncating the series (2.81) and the employment of the estimated coordinates in the truncated series.

Chapter 3

Discrete Time Systems

In the preceding chapter active vibration control of continuous time systems was considered. The control analysis was performed on the following implicit assumptions

- The state vector containing displacement- and velocity components is available for continuous time and noise free measuring.

- The control forces $F_\alpha(t)$, $\alpha = 1, .., n_m$ can be calculated on the basis of the measured state variables at the time t and applied to the structure at the same time.

Consider the case, where the measured signal is an acceleration, designated $\ddot{Z}_\alpha(t)$. $Z_\alpha(t)$ and $\dot{Z}_\alpha(t)$ can then be calculated by numerical integration. When $Z_\alpha(t)$ and $\dot{Z}_\alpha(t)$ are determined in this way they are encumbered with errors because of measurement errors in $\ddot{Z}_\alpha$ and local truncation errors in the employed numerical integration scheme, respectively. Indeed, $\ddot{Z}_\alpha(t)$ can only be measured at discrete equidistant instants t=kh, $k = 0, 1, ...$ These limitations are the same concerning sampling of the earthquake excitation $\{\ddot{\mathbf{u}}^{(0)}(t), \ t \in [t_0, T[\}$.

In practice there will be a time delay between the measured variables $\ddot{Z}_\alpha(t)$ and the application of the corrective forces, $F_\alpha(t)$. The time delay is due to on-line calculations such as numerical integration of the acceleration signals and calculation of control signals. Further, inertia in the moving parts of the actuators results in time delay.

In this chapter it is assumed that the total time delay caused by on-line calculations and inertia in the actuators is less than one sampling period h. In chapter 4 a control algorithm is described in which the time delay is longer than one sampling period h, and the on-line calculations are less than h.

In active control a common situation is that the measurements are received by a computer via an A-D converter, and the control signals are transmitted from the same computer via an D-A converter. Normally, the D-A converter is constructed so that it holds the analog signal constant until a new conversion is commanded. Hence, the control signal is also specified at discrete times.

Subsequently, an optimal control law taking into account the above-mentioned practical problems is developed. The optimal discrete time control problem is first formulated and solved on the basis of the continuous time problem in chapter 2. Next, the problem concerning time delay and measuring noise is treated.

3.1 Discrete Time Optimal Control

Discrete time control can be carried out by discretization of the state space equation (2.13) and the Ricatti equations (2.27)-(2.29) using a difference scheme. Hereby, errors are introduced in the control law caused by local truncation errors in the difference operator. In what follows the exact difference equations for the state space - and Ricatti equations are set up on the assumption of constant earthquake excitations and control forces between the sampling instants.

The external excitations and the control signals are specified by discontinuous functions with the convention that they are continuous from the right, i.e. $\ddot{\mathbf{u}}^{(0)}(t) = \ddot{\mathbf{u}}^{(0)}(t_0+kh)$ and $\mathbf{F}(t) = \mathbf{F}(t_0+kh)$ in the interval $t \in [t_0+kh, t_0+(k+1)h[$.

The interval $[t_0, T[$ is split up into N equivalent intervals with the length h. Given the state at the sampling time t_k the state at some future time $t \geq t_0+kh$ is obtained by solving (2.13)

$$\mathbf{Y}(t) = \boldsymbol{\Theta}(t, t_0+kh)\mathbf{Y}(t_0+kh) + \int_{t_0+kh}^{t} \boldsymbol{\Theta}(t, \tau) \left(\mathbf{B}_1 \ddot{\mathbf{u}}^{(0)}(\tau) + \mathbf{B}_2 \mathbf{F}(\tau) \right) d\tau \tag{3.1}$$

where $\boldsymbol{\Theta}(t, \tau)$ is the fundamental matrix of (2.13) satisfying

$$\frac{d}{dt}\boldsymbol{\Theta}(t, \tau) = \mathbf{A}(t)\boldsymbol{\Theta}(t, \tau), \ t > \tau, \quad \boldsymbol{\Theta}(\tau, \tau) = \mathbf{E} \tag{3.2}$$

Assuming that the earthquake excitations and the control signals are constant between the sampling instants, one obtains

$$\begin{aligned} \mathbf{Y}(t) &= \boldsymbol{\Theta}(t, t_0+kh)\mathbf{Y}(t_0+kh) + \mathbf{b}_1(t, t_0+kh)\ddot{\mathbf{u}}^{(0)}(t_0+kh) \\ &+ \mathbf{b}_2(t, t_0+kh)\mathbf{F}(t_0+kh), \quad t \in]t_0+kh, t_0+(k+1)h] \end{aligned} \tag{3.3}$$

where

$$\mathbf{b}_1(t, t_0+kh) = \int_{t_0+kh}^{t} \boldsymbol{\Theta}(t, \tau)\mathbf{B}_1 d\tau \tag{3.4}$$

$$\mathbf{b}_2(t, t_0+kh) = \int_{t_0+kh}^{t} \boldsymbol{\Theta}(t, \tau)\mathbf{B}_2 d\tau \tag{3.5}$$

The states at the next sampling time $t = t_0+(k+1)h$ are thus given by

$$\begin{aligned} \mathbf{Y}(t_0+(k+1)h) &= \boldsymbol{\Theta}(t_0+(k+1)h, t_0+kh)\mathbf{Y}(t_0+kh) \\ &+ \mathbf{b}_1(t_0+(k+1)h, t_0+kh)\ddot{\mathbf{u}}^{(0)}(t_0+kh) \\ &+ \mathbf{b}_2(t_0+(k+1)h, t_0+kh)\mathbf{F}(t_0+kh) \end{aligned} \tag{3.6}$$

(3.6) constitutes the difference scheme searched for.

3.1.1 Determination of the Optimal Control Forces

The performance index (2.18) can be written in the form

$$J(\mathbf{Y}(t_0), t_0) = \frac{1}{2}\mathbf{Y}^T(t_0+Nh)\mathbf{S}(t_0+Nh)\mathbf{Y}(t_0+Nh) + \frac{1}{2}\sum_{k=0}^{N-1} J^{(k)} \tag{3.7}$$

where

$$J^{(k)} = \int_{t_0+kh}^{t_0+(k+1)h} \left(\mathbf{Y}^T(\tau)\mathbf{Q}(\tau)\mathbf{Y}(\tau) + \mathbf{F}^T(\tau)\mathbf{R}(\tau)\mathbf{F}(\tau) \right) d\tau \tag{3.8}$$

Using (1.3) in (1.8) gives

$$
\begin{aligned}
J^{(k)} = {} & \mathbf{Y}^T(t_0+kh)\mathbf{Q}_{00}^{(k)}\mathbf{Y}(t_0+kh) + \mathbf{F}^T(t_0+kh)\mathbf{R}_{22}^{(k)}\mathbf{F}(t_0+kh) \\
& + \ddot{\mathbf{u}}^{(0)T}(t_0+kh)\mathbf{Q}_{11}^{(k)}\ddot{\mathbf{u}}^{(0)}(t_0+kh) + 2\mathbf{Y}^T(t_0+kh)\mathbf{Q}_{01}^{(k)}\ddot{\mathbf{u}}^{(0)}(t_0+kh) \\
& + 2\mathbf{Y}^T(t_0+kh)\mathbf{Q}_{02}^{(k)}\mathbf{F}(t_0+kh) + 2\ddot{\mathbf{u}}^{(0)T}(t_0+kh)\mathbf{Q}_{12}^{(k)}\mathbf{F}(t_0+kh)
\end{aligned}
\tag{3.9}
$$

where

$$
\mathbf{Q}_{00}^{(k)} = \int_{t_0+kh}^{t_0+(k+1)h} \boldsymbol{\Theta}^T(\tau,t_0+kh)\mathbf{Q}(\tau)\boldsymbol{\Theta}(\tau,t_0+kh)\mathrm{d}\tau
\tag{3.10}
$$

$$
\mathbf{Q}_{11}^{(k)} = \int_{t_0+kh}^{t_0+(k+1)h} \mathbf{b}_1^T(\tau,t_0+kh)\mathbf{Q}(\tau)\mathbf{b}_1(\tau,t_0+kh)\mathrm{d}\tau
\tag{3.11}
$$

$$
\mathbf{Q}_{12}^{(k)} = \int_{t_0+kh}^{t_0+(k+1)h} \mathbf{b}_1^T(\tau,t_0+kh)\mathbf{Q}(\tau)\mathbf{b}_2(\tau,t_0+kh)\mathrm{d}\tau
\tag{3.12}
$$

$$
\mathbf{Q}_{01}^{(k)} = \int_{t_0+kh}^{t_0+(k+1)h} \boldsymbol{\Theta}^T(\tau,t_0+kh)\mathbf{Q}(\tau)\mathbf{b}_1(\tau,t_0+kh)\mathrm{d}\tau
\tag{3.13}
$$

$$
\mathbf{Q}_{02}^{(k)} = \int_{t_0+kh}^{t_0+(k+1)h} \boldsymbol{\Theta}^T(\tau,t_0+kh)\mathbf{Q}(\tau)\mathbf{b}_2(\tau,t_0+kh)\mathrm{d}\tau
\tag{3.14}
$$

$$
\mathbf{R}_{22}^{(k)} = \int_{t_0+kh}^{t_0+(k+1)h} \left(\mathbf{b}_2^T(\tau,t_0+kh)\mathbf{Q}(\tau)\mathbf{b}_2(\tau,t_0+kh) + \mathbf{R}(\tau) \right) \mathrm{d}\tau
\tag{3.15}
$$

Then the performance index is

$$
\begin{aligned}
J = {} & J(\mathbf{Y}(t_0),t_0) \\
= {} & \frac{1}{2}\mathbf{Y}^T(t_0+Nh)\mathbf{S}(t_0+Nh)\mathbf{Y}(t_0+Nh) \\
& + \frac{1}{2}\sum_{k=0}^{N-1} \Big(\mathbf{Y}^T(t_0+kh)\mathbf{Q}_{00}^{(k)}\mathbf{Y}(t_0+kh) + \mathbf{F}^T(t_0+kh)\mathbf{R}_{22}^{(k)}\mathbf{F}(t_0+kh) \\
& + \ddot{\mathbf{u}}^{(0)T}(t_0+kh)\mathbf{Q}_{11}^{(k)}\ddot{\mathbf{u}}^{(0)}(t_0+kh) + 2\mathbf{Y}^T(t_0+kh)\mathbf{Q}_{01}^{(k)}\ddot{\mathbf{u}}(t_0+kh) \\
& + 2\mathbf{Y}^T(t_0+kh)\mathbf{Q}_{02}^{(k)}\mathbf{F}(t_0+kh) + 2\ddot{\mathbf{u}}^{(0)T}(t_0+kh)\mathbf{Q}_{12}^{(k)}\mathbf{F}(t_0+kh) \Big)
\end{aligned}
\tag{3.16}
$$

The objective is to determine the control sequence $\{\mathbf{F}^*(t_0+kh),\ k=0,..,N-1\}$ to minimize (1.16). Next, the state sequence $\{\mathbf{Y}^*(t_0+kh),\ k=0,..,N-1\}$ is determined from (1.6).

The initial time t_0 is considered as a variable. The optimal performance index $J^*(T-kh)$, $k=1,..,N$ is determined stage-by-stage from the final time T. For $t=T$ the final condition is given according to (2.24)

$$
J^*(\mathbf{Y}(T),T) = \frac{1}{2}\mathbf{Y}^T(T)\mathbf{S}_T\mathbf{Y}(T)
\tag{3.17}
$$

Assume that the minimum cost of the process $J^*(\mathbf{y}, T-(k-1)h)$, $k = 1, .., N$, starting at $t = T-(k-1)h$ is known for all values of the state vector $\mathbf{y} \in R^n$. Hence, for $t = T-kh$ the optimal performance index can be written as

$$
\begin{aligned}
J^* &= J^*(\mathbf{Y}(T-kh), T-kh) \\
&= \min_{\mathbf{F}(T-kh)} \left(\frac{1}{2} \mathbf{Y}^T(T-kh) \mathbf{Q}_{00}^{(N-k)} \mathbf{Y}(T-kh) \right. \\
&\quad + \frac{1}{2} \mathbf{F}^T(T-kh) \mathbf{R}_{22}^{(N-k)} \mathbf{F}(T-kh) + \frac{1}{2} \ddot{\mathbf{u}}^{(0)T}(T-kh) \mathbf{Q}_{11}^{(N-k)} \ddot{\mathbf{u}}^{(0)}(T-kh) \\
&\quad + \mathbf{Y}^T(T-kh) \mathbf{Q}_{01}^{(N-k)} \ddot{\mathbf{u}}^{(0)}(T-kh) + \mathbf{Y}^T(T-kh) \mathbf{Q}_{02}^{(N-k)} \mathbf{F}(T-kh) \\
&\quad \left. + \ddot{\mathbf{u}}^{(0)T}(T-kh) \mathbf{Q}_{12}^{(N-k)} \mathbf{F}(T-kh) + J^*(\mathbf{Y}(T-(k-1)h), T-(k-1)h) \right)
\end{aligned}
$$
$$(3.18)$$

Eq. (1.18) is solved by assuming a solution for arbitrary $\mathbf{y} \in R^n$, given by

$$
\begin{aligned}
J^* &= J^*(\mathbf{y}, T-kh) \\
&= \frac{1}{2} \mathbf{y}^T \mathbf{S}(T-kh) \mathbf{y} + \mathbf{y}^T \mathbf{T}(T-kh) + V(T-kh), \quad k = 0, .., N
\end{aligned}
$$
$$(3.19)$$

where $\mathbf{S}$, $\mathbf{T}$ and V are an $n \times n$ positive definite symmetric matrix, an $n \times 1$ vector, and a scalar, respectively. They will be selected so as to force (1.19) to satisfy (1.18).

First (1.19) is inserted into the right hand side of (1.18), and next (1.6) is used to eliminate $\mathbf{Y}(T-(k-1)h)$. Since there are no restrictions on $\mathbf{F}(T-kh)$, the minimizing $\mathbf{F}(T-kh)$ is then found by setting the gradient with respect to $\mathbf{F}(T-kh)$ equal to zero. After some calculations this yields

$$
\begin{aligned}
\mathbf{F}^*(T-kh) &= -\mathbf{Q}_{22}^{(N-k)} \left(\left(\mathbf{Q}_{02}^{(N-k)T} + \mathbf{b}_2^T(T-(k-1)h, T-kh) \right. \right. \\
&\quad \left. \mathbf{S}(T-(k-1)h) \Theta(T-(k-1)h, T-kh) \right) \mathbf{Y}(T-kh) \\
&\quad + \left(\mathbf{Q}_{12}^{(N-k)T} + \mathbf{b}_2^T(T-(k-1)h, T-kh) \mathbf{S}(T-(k-1)h) \right. \\
&\quad \left. \mathbf{b}_1(T-(k-1)h, T-kh) \right) \ddot{\mathbf{u}}^{(0)}(T-kh) \\
&\quad \left. \mathbf{b}_2^T(T-(k-1)h, T-kh) \mathbf{T}(T-(k-1)h) \right)
\end{aligned}
$$
$$(3.20)$$

where

$$
\begin{aligned}
\mathbf{Q}_{22}^{(N-k)} &= \left(\mathbf{R}_{22}^{(N-k)} + \mathbf{b}_2^T(T-(k-1)h, T-kh) \right. \\
&\quad \left. \mathbf{S}(T-(k-1)h) \mathbf{b}_2(T-(k-1)h, T-kh) \right)^{-1}
\end{aligned}
$$
$$(3.21)$$

After rearranging and simplifying, this gives

$$
\begin{aligned}
J^* \;=\;& J^*(\mathbf{y}, T{-}kh) \\[4pt]
=\;& \tfrac{1}{2}\mathbf{y}^T \Bigg(\Big(\mathbf{Q}_{00}^{(N-k)} + \boldsymbol{\Theta}^T(T{-}(k{-}1)h, T{-}kh)\mathbf{S}(T{-}(k{-}1)h)\boldsymbol{\Theta}(T{-}(k{-}1)h, T{-}kh) \Big) \\[4pt]
&- \Big(\mathbf{Q}_{02}^{(N-k)} + \boldsymbol{\Theta}^T(T{-}(k{-}1)h, T{-}kh)\mathbf{S}(T{-}(k{-}1)h)\mathbf{b}_2(T{-}(k{-}1)h, T{-}kh) \Big) \mathbf{Q}_{22}^{(N-k)} \\[4pt]
&\Big(\mathbf{Q}_{02}^{(N-k)T} + \mathbf{b}_2^T(T{-}(k{-}1)h, T{-}kh)\mathbf{S}(T{-}(k{-}1)h)\boldsymbol{\Theta}(T{-}(k{-}1)h, T{-}kh) \Big) \Bigg) \mathbf{y} \\[6pt]
+\;& \mathbf{y}^T \Bigg(\Big(\big(\mathbf{Q}_{01}^{(N-k)} + \boldsymbol{\Theta}^T(T{-}(k{-}1)h, T{-}kh)\mathbf{S}(T{-}(k{-}1)h)\mathbf{b}_1(T{-}(k{-}1)h, T{-}kh) \big) \\[4pt]
&- \Big(\mathbf{Q}_{02}^{(N-k)} + \boldsymbol{\Theta}^T(T{-}(k{-}1)h, T{-}kh)\mathbf{S}(T{-}(k{-}1)h)\mathbf{b}_2(T{-}(k{-}1)h, T{-}kh) \Big) \mathbf{Q}_{22}^{(N-k)} \\[4pt]
&\Big(\mathbf{Q}_{12}^{(N-k)T} + \mathbf{b}_2^T(T{-}(k{-}1)h, T{-}kh)\mathbf{S}(T{-}(k{-}1)h)\mathbf{b}_1(T{-}(k{-}1)h, T{-}kh) \Big) \Big) \ddot{\mathbf{u}}^{(0)}(T{-}kh) \\[6pt]
+\;& \Big(\boldsymbol{\Theta}^T(T{-}(k{-}1)h, T{-}kh) - \Big(\mathbf{Q}_{02}^{(N-k)} \\[4pt]
+\;& \boldsymbol{\Theta}^T(T{-}(k{-}1)h, T{-}kh)\mathbf{S}(T{-}(k{-}1)h)\mathbf{b}_2(T{-}(k{-}1)h, T{-}kh) \Big) \\[4pt]
&\mathbf{Q}_{22}^{(N-k)}\mathbf{b}_2^T(T{-}(k{-}1)h, T{-}kh) \Big) \mathbf{T}(T{-}(k{-}1)h) \Bigg) \\[6pt]
+\;& \tfrac{1}{2}\ddot{\mathbf{u}}^{(0)T}(T{-}kh) \Bigg(\Big(\mathbf{Q}_{11}^{(N-k)} + \mathbf{b}_1^T(T{-}(k{-}1)h, T{-}kh)\mathbf{S}(T{-}(k{-}1)h)\mathbf{b}_1(T{-}(k{-}1)h, T{-}kh) \Big) \\[4pt]
&- \Big(\mathbf{Q}_{12}^{(N-k)} + \mathbf{b}_1^T(T{-}(k{-}1)h, T{-}kh)\mathbf{S}(T{-}(k{-}1)h)\mathbf{b}_2(T{-}(k{-}1)h, T{-}kh) \Big) \mathbf{Q}_{22}^{(N-k)} \\[4pt]
&\Big(\mathbf{Q}_{12}^{(N-k)T} + \mathbf{b}_2^T(T{-}(k{-}1)h, T{-}kh)\mathbf{S}(T{-}(k{-}1)h)\mathbf{b}_1(T{-}(k{-}1)h, T{-}kh) \Big) \Bigg) \ddot{\mathbf{u}}^{(0)}(T{-}kh) \\[6pt]
-\;& \ddot{\mathbf{u}}^{(0)T}(T{-}kh) \Big(\mathbf{Q}_{12}^{(N-k)} + \mathbf{b}_1^T(T{-}(k{-}1)h, T{-}kh)\mathbf{S}(T{-}(k{-}1)h)\mathbf{b}_2(T{-}(k{-}1)h, T{-}kh) \Big) \\[4pt]
&\mathbf{Q}_{22}^{(N-k)}\mathbf{b}_2^T(T{-}(k{-}1)h, T{-}kh) - \mathbf{b}_1^T(T{-}(k{-}1)h, T{-}kh) \Big) \mathbf{T}(T{-}(k{-}1)h) \\[6pt]
-\;& \tfrac{1}{2}\mathbf{T}^T(T{-}(k{-}1)h)\mathbf{b}_2(T{-}(k{-}1)h, T{-}kh)\mathbf{Q}_{22}^{(N-k)}\mathbf{b}_2^T(T{-}(k{-}1)h, T{-}kh)\mathbf{T}(T{-}(k{-}1)h) \\[4pt]
+\;& V(T{-}(k{-}1)h) \tag{3.22}
\end{aligned}
$$

Substituting (3.19) into (3.22) and equating the left-hand and right-hand sides, the assumed form for $J^*(\mathbf{y}, T{-}kh)$ can be forced to be the solution for all $\mathbf{y} \in R^n$ by requiring that the quadratic terms, the linear terms, and the terms not involving $\mathbf{y}$ all balance individually. This requires

$$\mathbf{S}(T-kh) =$$
$$\left(\mathbf{Q}_{00}^{(N-k)} + \Theta^T(T-(k-1)h, T-kh)\mathbf{S}(T-(k-1)h)\Theta(T-(k-1)h, T-kh) \right)$$
$$- \left(\mathbf{Q}_{02}^{(N-k)} + \Theta^T(T-(k-1)h, T-kh)\mathbf{S}(T-(k-1)h)\mathbf{b}_2(T-(k-1)h, T-kh) \right) \mathbf{Q}_{22}^{(N-k)}$$
$$\left(\mathbf{Q}_{02}^{(N-k)T} + \mathbf{b}_2^T(T-(k-1)h, T-kh)\mathbf{S}(T-(k-1)h)\Theta(T-(k-1)h, T-kh) \right) \qquad (3.23)$$

$$\mathbf{T}(T-kh) =$$
$$\left(\left(\mathbf{Q}_{01}^{(N-k)} + \Theta^T(T-(k-1)h, T-kh)\mathbf{S}(T-(k-1)h)\mathbf{b}_1(T-(k-1)h, T-kh) \right) \right.$$
$$- \left(\mathbf{Q}_{02}^{(N-k)} + \Theta^T(T-(k-1)h, T-kh)\mathbf{S}(T-(k-1)h)\mathbf{b}_2(T-(k-1)h, T-kh) \right) \mathbf{Q}_{22}^{(N-k)}$$
$$\left. \left(\mathbf{Q}_{12}^{(N-k)T} + \mathbf{b}_2^T(T-(k-1)h, T-kh)\mathbf{S}(T-(k-1)h)\mathbf{b}_1(T-(k-1)h, T-kh) \right) \right) \ddot{\mathbf{u}}^{(0)}(T-kh)$$
$$+ \left(\Theta^T(T-(k-1)h, T-kh) - \left(\mathbf{Q}_{02}^{(N-k)T} \right. \right.$$
$$+ \left. \Theta^T(T-(k-1)h, T-kh)\mathbf{S}(T-(k-1)h)\mathbf{b}_2(T-(k-1)h, T-kh) \right)$$
$$\left. \mathbf{Q}_{22}^{(N-k)}\mathbf{b}_2^T(T-(k-1)h, T-kh) \right) \mathbf{T}(T-(k-1)h) \qquad (3.24)$$

$$V(T-kh) =$$
$$\frac{1}{2}\ddot{\mathbf{u}}^{(0)T}(T-kh) \left(\left(\mathbf{Q}_{11}^{(N-k)} + \mathbf{b}_1^T(T-(k-1)h, T-kh)\mathbf{S}(T-(k-1)h)\mathbf{b}_1(T-(k-1)h, T-kh) \right) \right.$$
$$- \left(\mathbf{Q}_{12}^{(N-k)} + \mathbf{b}_1^T(T-(k-1)h, T-kh)\mathbf{S}(T-(k-1)h)\mathbf{b}_2(T-(k-1)h, T-kh) \right) \mathbf{Q}_{22}^{(N-k)}$$
$$\left. \left(\mathbf{Q}_{12}^{(N-k)T} + \mathbf{b}_2^T(T-(k-1)h, T-kh)\mathbf{S}(T-(k-1)h)\mathbf{b}_1(T-(k-1)h, T-kh) \right) \right) \ddot{\mathbf{u}}^{(0)}(T-kh)$$
$$- \ddot{\mathbf{u}}^{(0)T}(T-kh) \left(\mathbf{Q}_{12}^{(N-k)} + \mathbf{b}_1^T(T-(k-1)h, T-kh)\mathbf{S}(T-(k-1)h)\mathbf{b}_2(T-(k-1)h, T-kh) \right)$$
$$\left. \mathbf{Q}_{22}^{(N-k)}\mathbf{b}_2^T(T-(k-1)h, T-kh) - \mathbf{b}_1^T(T-(k-1)h, T-kh) \right) \mathbf{T}(T-(k-1)h)$$
$$- \frac{1}{2}\mathbf{T}^T(T-(k-1)h)\mathbf{b}_2(T-(k-1)h, T-kh)\mathbf{Q}_{22}^{(N-k)}\mathbf{b}_2^T(T-(k-1)h, T-kh)\mathbf{T}(T-(k-1)h)$$
$$+ V(T-(k-1)h) \qquad (3.25)$$

The final conditions for (3.23)-(3.25) are $\mathbf{S}(T) = \mathbf{S}_T$, $\mathbf{T}(T) = \mathbf{0}$ and $V(T) = 0$.

(3.23)-(3.25) are the exact difference equations for (2.27)-(2.29). (3.23) is the *discrete time Ricatti equation*.

In order to determine the optimal control force $\mathbf{F}^*(t_0+kh)$ given by (3.20), (3.23) is solved first, and next (3.24). Actually, (3.25) never needs to be solved if the only interest is finding the optimal control. $V(t_0+kh)$ is only needed if J^* has to be calculated.

Assume $\ddot{\mathbf{u}}^{(0)}(t_0+kh) = \mathbf{0}$, $k = 0,..,N-1$, corresponding an autonomous system. Then (3.24) is a homogeneous equation with zero initial conditions $\mathbf{T}(T) = \mathbf{0}$, so $\mathbf{T}(t_0+kh) = \mathbf{0}$, $k = 0,..,N-1$. Additionally, $V(t_0+kh) = 0$, $k = 0,..,N-1$.

According to (3.22), when an autonomous system is considered, the optimal cost at any time in the interval $[t_0+kh, T]$, $k = 0,..,N-1$, is seen to be

$$\forall\, \mathbf{y} \in R^n \,:\, J^*(\mathbf{y}, t_0+kh) = \frac{1}{2}\mathbf{y}^T\mathbf{S}(t_0+kh)\mathbf{y} \tag{3.26}$$

The optimal control law given by (3.20) has the same form as the continuous time control law (2.32). Thus, the optimal control force is composed of a closed-loop part depending on the current state and an open-loop part depending on the external loading. In what follows only the closed-loop control is considered. This is only optimal by free vibrations. In other cases the limitations described in section 2.2.1 are the same.

To facilitate, define a feedback gain sequence as

$$\begin{aligned}
\mathbf{G}(t_0+kh) \;=\;& \mathbf{Q}_{22}^{(k)}\left(\mathbf{Q}_{02}^{(k)T} + \mathbf{b}_2^T(t_0+(k+1)h, t_0+kh)\right. \\[2mm]
& \left. \mathbf{S}(t_0+(k+1)h)\mathbf{\Theta}(t_0+(k+1)h, t_0+kh)\right)
\end{aligned} \tag{3.27}$$

so that the closed-loop control force given by (3.20) can be written in the form

$$\mathbf{F}^{(c)}(t_0+kh) = -\mathbf{G}(t_0+kh)\mathbf{Y}^{(c)}(t_0+kh) \tag{3.28}$$

3.1.2 Steady-State Feedback Gains

A time-invariant structure matrix $\mathbf{A}$ is assumed. Hereby, the fundamental matrix of (2.13) can be written as, cf. (3.2)

$$\mathbf{\Theta}(t,\tau) = \exp(\mathbf{A}(t-\tau)),\; t \geq \tau \tag{3.29}$$

where

$$\exp(\mathbf{A}t) = \mathbf{E} + \mathbf{A}t + \frac{1}{2!}\mathbf{A}\mathbf{A}t^2 + \cdots \tag{3.30}$$

As an alternative to the Maclaurin series (3.30) $\exp(\mathbf{A}t)$ can be calculated from

$$\exp(\mathbf{A}t) = \mathbf{\Phi}\exp(\mathbf{\Lambda}t)\mathbf{\Phi}^{-1} \tag{3.31}$$

$\mathbf{\Phi}$ and $\exp(\mathbf{\Lambda}t)$ are an $n \times n$ dimensional modal matrix and a diagonal matrix, respectively, defined as

$$\mathbf{\Phi} = [\,\mathbf{\Phi}^{(1)} \quad \cdot \quad \cdot \quad \cdot \quad \mathbf{\Phi}^{(n)}\,] \tag{3.32}$$

$$\exp(\mathbf{\Lambda}t) = \begin{bmatrix} \exp(\lambda_1 t) & & & \\ & \cdot & & \\ & & \cdot & \\ & & & \cdot & \\ & & & & \exp(\lambda_n t) \end{bmatrix} \tag{3.33}$$

$\lambda_i, \Phi^{(i)}$ are eigenvalues and eigenvectors to $\mathbf{A}$

$$\mathbf{A}\Phi^{(i)} = \lambda_i \Phi^{(i)}, \; i = 1, .., n \tag{3.34}$$

Since $\mathbf{A}$ is non-symmetric, λ_i and $\Phi^{(i)}$ are normally complex.

In this case $\Theta(t, \tau)$ only depends on t and τ through the difference $t - \tau$. Thus, we have

$$\Theta(t_0 + (k+1)h, t_0 + kh) = \Theta(h, 0) = \exp(\mathbf{A}h) \tag{3.35}$$

$$\mathbf{b}_1(t_0 + (k+1)h, t_0 + kh) = \mathbf{b}_1(h, 0) = \mathbf{A}^{-1}(\exp(\mathbf{A}h) - \mathbf{E})\mathbf{B}_1 \tag{3.36}$$

$$\mathbf{b}_2(t_0 + (k+1)h, t_0 + kh) = \mathbf{b}_2(h, 0) = \mathbf{A}^{-1}(\exp(\mathbf{A}h) - \mathbf{E})\mathbf{B}_2 \tag{3.37}$$

Furthermore, the matrices $\mathbf{Q}$ and $\mathbf{R}$ are assumed to be time-invariant, so that the system matrices (3.10)-(3.15) are time-invariant. For that reason the upper index (k) is omitted in the remainder.

(3.23) is solved backward in time beginning at time T. As $T \to \infty$ the sequence $\mathbf{S}$ may under certain conditions converge to a steady-state matrix $\mathbf{S}(\infty)$.

If $\mathbf{S}$ does converge, then for large T, evidently $\mathbf{S}(\infty) \equiv \mathbf{S}(T - kh) = \mathbf{S}(T - (k-1)h)$. The steady-state solution of the discrete time Ricatti equation (3.23) is thus determined from the system of non-linear equations

$$\begin{aligned} \mathbf{S} = \; & \mathbf{Q}_{00} + \Theta^T(h, 0)\mathbf{S}\Theta(h, 0) \\ & - \left(\mathbf{Q}_{02} + \Theta^T(h, 0)\mathbf{S}\mathbf{b}_2(h, 0) \right) \left(\mathbf{R}_{22} + \mathbf{b}_2^T(h, 0)\mathbf{S}\mathbf{b}_2(h, 0) \right)^{-1} \\ & \left(\mathbf{Q}_{02}^T + \mathbf{b}_2^T(h, 0)\mathbf{S}\Theta(h, 0) \right) \end{aligned} \tag{3.38}$$

(3.38) represents the Lyapunov equation concerning discrete time systems. Like the continuous time formulation (2.42), (3.38) represents $n(n+1)/2$ non-linear equations which have to be solved by iteration. For $n = 2$ the analytical solution from the continuous-time system (2.79) can be used as a starting value by the iteration. Generally, more than one solution of the quadratic equation (3.38) exist. The extraneous roots can usually be eliminated by the requirement that $\mathbf{S}$ must be positive semi-definite.

If the limiting solution exists then the corresponding steady-state feedback gain is

$$\mathbf{G}(\infty) = \left(\mathbf{R}_{22} + \mathbf{b}_2^T(h, 0)\mathbf{S}(\infty)\mathbf{b}_2(h, 0) \right)^{-1} \left(\mathbf{Q}_{02}^T + \mathbf{b}_2^T(h, 0)\mathbf{S}(\infty)\Theta(h, 0) \right) \tag{3.39}$$

The following time-invariant, closed-loop control law can then be used

$$\mathbf{F}^{(c)}(t_0 + kh) = -\mathbf{G}(\infty)\mathbf{Y}^{(c)}(t_0 + kh) \tag{3.40}$$

3.2 Measuring Noise and Time Delay

In practice the control law (3.28) is not applicable, since the state vector $\mathbf{Y}(t_0 + kh)$ cannot be determined exactly by direct measuring and the control forces cannot be applied to the structure at the same time as the measurings are made. Thus, a control law is introduced in which the control force is based on an estimate of the state vector at the time where the control force can be applied.

The measurements, $\mathbf{Z}(t_0+kh)$, made while the system is in stage t_0+kh, are assumed to be linearly related to the state $\mathbf{Y}(t_0+kh)$ by

$$\mathbf{Z}(t_0+kh) = \mathbf{D}\mathbf{Y}(t_0+kh) + \mathbf{e}(t_0+kh) \tag{3.41}$$

$\mathbf{D} \in R^{n \times n}$ is a time-invariant transformation matrix and $\{\mathbf{e}(t_0+kh), \ k = 0, .., N-1\}$ is a *white Gaussian random sequence*, which means that $\mathbf{e}(t_0+kh)$ is a normally distributed stochastic vector, fulfilling

$$\forall \ k = 0, .., N-1 : \quad E[\mathbf{e}(t_0+kh)] = \mathbf{0} \tag{3.42}$$

$$\forall \ k, l = 0, .., N-1 :$$
$$E[\mathbf{e}(t_0+kh)\mathbf{e}^T(t_0+lh)] = \begin{cases} \mathbf{0}, & l \neq k \\ \mathbf{R}_\mathbf{e}(t_0+kh), & l = k \end{cases} \tag{3.43}$$

The white Gaussian random sequence is designated stationary if the covariance matrix $\mathbf{R_e} \in R^{n \times n}$ does not depend on k, which is assumed.

Besides, it is assumed that $\{\ddot{\mathbf{u}}^{(0)}(t_0+kh), \ k = 0, .., N-1\}$ in the difference equation (3.6) is a non-stationary white Gaussian random sequence, which implies

$$\forall \ k = 0, .., N-1 : \quad E[\ddot{\mathbf{u}}^{(0)}(t_0+kh)] = \mathbf{0} \tag{3.44}$$

$$\forall \ k, l = 0, .., N-1 :$$
$$E[\ddot{\mathbf{u}}^{(0)}(t_0+kh)\ddot{\mathbf{u}}^{(0)T}(t_0+lh)] = \begin{cases} \mathbf{0}, & l \neq k \\ \mathbf{R}_{\ddot{\mathbf{u}}^{(0)}}(t_0+kh), & l = k \end{cases} \tag{3.45}$$

$$\forall \ k, l = 0, .., N-1 :$$
$$E[\ddot{\mathbf{u}}^{(0)}(t_0+kh)\mathbf{e}^T(t_0+lh)] = \begin{cases} \mathbf{0}, & l \neq k \\ \mathbf{R}_{\ddot{\mathbf{u}}^{(0)}\mathbf{e}}(t_0+kh), & l = k \end{cases} \tag{3.46}$$

Since the earthquake excitation is non-stationary the covariance matrix $\mathbf{R}_{\ddot{\mathbf{u}}^{(0)}}(t_0+kh) \in R^{3 \times 3}$ in (3.45) and $\mathbf{R}_{\ddot{\mathbf{u}}^{(0)}\mathbf{e}}(t_0+kh) \in R^{3 \times n}$ in (3.46) depends on time.

Next, the object is to make a good estimate $\hat{\mathbf{Y}}(t_0 + (k + m)h|t_0+kh), \ m \in R_+$ of $\mathbf{Y}(t_0 + (k + m)h)$ from measurements $\{\mathbf{Z}(t_0 + jh), \ j = 0, .., k\}$ up to time t_0+kh, which are imprecise and only functions of the state variables, knowing, too, that the system itself is subjected to random disturbances in the interval $[t_0+(k+1)h, t_0 + (k + m)h[$. The notation $\hat{\mathbf{Y}}(t_0 + (k + m)h|t_0+kh)$ is used to indicate, that it is an estimate based on measurements available from the time interval $[t_0, t_0+kh]$. This is a prediction problem and the resulting dynamic system for the estimated state is called a filter.

3.2.1 Kalman Filter

In the prediction problem, consider the structure described by the linear stochastic difference equation (3.6), where

$$\forall \ k = 0, .., N-1 : \quad E[\mathbf{Y}(t_0+kh)] = \bar{\mathbf{Y}}^{(k)} \tag{3.47}$$

$$\forall \ k = 0, .., N-1 :$$
$$E\left[\left(\mathbf{Y}(t_0+kh) - \bar{\mathbf{Y}}^{(k)}\right)\left(\mathbf{Y}(t_0+kh) - \bar{\mathbf{Y}}^{(k)}\right)^T\right] = \mathbf{R_Y}(t_0+kh) \tag{3.48}$$

$$\forall\, k = 0, .., N-1: \quad E\left[\mathbf{Y}(t_0+kh)\ddot{\mathbf{u}}^{(0)T}(t_0+kh)\right] = \mathbf{0} \tag{3.49}$$

$$\forall\, k = 0, .., N-1: \quad E\left[\mathbf{Y}(t_0+kh)\mathbf{e}^T(t_0+kh)\right] = \mathbf{0} \tag{3.50}$$

(3.49) is due to (3.6) which states that $\mathbf{Y}(t_0{+}kh)$ is generated by the sequence $\{\ddot{\mathbf{u}}(t_0 + jh),\ j = 0, .., k - 1\}$ and therefore, $\mathbf{Y}(t_0{+}kh)$ and $\ddot{\mathbf{u}}(t_0{+}kh)$ are stochastically independent.

It is assumed that the the measuring noise and the excitation are uncorrelated, which means that $\mathbf{R}_{\ddot{\mathbf{u}}^{(0)}\mathbf{e}} = \mathbf{0}$.

Let the estimator have the form

$$\hat{\mathbf{Y}}(t_0{+}(k{+}m)h|t_0{+}kh)$$
$$= \boldsymbol{\Theta}(t_0{+}(k{+}m)h, t_0{+}kh)\hat{\mathbf{Y}}(t_0{+}kh|t_0{+}(k{-}1)h) + \int_{t_0+kh}^{t_0+(k+m)h} \boldsymbol{\Theta}(t,\tau)\mathbf{B}_2\mathbf{F}(\tau)\mathrm{d}\tau$$
$$+ \mathbf{H}(t_0{+}(k{+}m)h)\left(\mathbf{Z}(t_0{+}kh) - \mathbf{D}\hat{\mathbf{Y}}(t_0{+}kh|t_0{+}(k{-}1)h)\right) \tag{3.51}$$

Here $\mathbf{H}$ is a time dependent gain matrix, which has to be chosen in a suitable way. The term $\mathbf{Z} - \mathbf{D}\hat{\mathbf{Y}}$, is the difference between the measured and estimated outputs.

We shall look for a minimum-variance estimator, which refers to one minimizing the mean square estimation error. Introduce the estimation error

$$\Delta\mathbf{Y}(t_0{+}(k{+}m)h) = \mathbf{Y}(t_0{+}(k{+}m)h) - \hat{\mathbf{Y}}(t_0{+}(k{+}m)h|t_0{+}kh) \tag{3.52}$$

Inserting (3.1) for $t = t_0 + (k + m)h$, (3.41) and (3.51) into (3.52), and regrouping gives

$$\begin{aligned}
\Delta\mathbf{Y}(t_0{+}(k{+}m)h) = {} & \Big(\boldsymbol{\Theta}(t_0{+}(k{+}m)h, t_0{+}kh) \\
& - \mathbf{H}(t_0{+}(k{+}m)h)\mathbf{D}\Big)\Delta\mathbf{Y}(t_0{+}kh) \\
& + \int_{t_0+kh}^{t_0+(k+m)h} \boldsymbol{\Theta}(t,\tau)\mathbf{B}_1\ddot{\mathbf{u}}^{(0)}(\tau)\mathrm{d}\tau \\
& - \mathbf{H}(t_0{+}(k{+}m)h)\mathbf{e}(t_0{+}kh)
\end{aligned} \tag{3.53}$$

Introduce the variance of the estimation error, $\mathbf{P}(t_0{+}kh)$, defined as

$$\begin{aligned}
\mathbf{P}(t_0{+}kh) = {} & E\Big[\Big(\Delta\mathbf{Y}(t_0{+}kh) - E[\Delta\mathbf{Y}(t_0{+}kh)]\Big) \\
& \Big(\Delta\mathbf{Y}(t_0{+}kh) - E[\Delta\mathbf{Y}(t_0{+}kh)]\Big)^T\Big]
\end{aligned} \tag{3.54}$$

From (3.53) and by use of (3.4), (3.49) and (3.50), we have

$$\begin{aligned}
\mathbf{P} = {} & \mathbf{P}(t_0{+}(k{+}m)h) \\
= {} & E[\Delta\mathbf{Y}(t_0{+}(k{+}m)h)\Delta\mathbf{Y}^T(t_0{+}(k{+}m)h)] \\
= {} & \Big(\boldsymbol{\Theta}(t_0{+}(k{+}m)h, t_0{+}kh) - \mathbf{H}(t_0{+}(k{+}m)h)\mathbf{D}\Big)\mathbf{P}(t_0{+}kh) \\
& \Big(\boldsymbol{\Theta}(t_0{+}(k{+}m)h, t_0{+}kh) - \mathbf{H}(t_0{+}(k{+}m)h)\mathbf{D}\Big)^T \\
& + \mathbf{b}_1(t_0{+}(k{+}m)h, t_0{+}kh)\mathbf{R}_{\ddot{\mathbf{u}}^{(0)}}(t_0{+}kh)\mathbf{b}_1^T(t_0{+}(k{+}m)h, t_0{+}kh) \\
& + \mathbf{H}(t_0{+}(k{+}m)h)\mathbf{R_e}\mathbf{H}^T(t_0{+}(k{+}m)h),\ k = 0, .., N-1
\end{aligned} \tag{3.55}$$

The criterion for choosing the unknown matrix $\mathbf{H}(t_0+(k+m)h)$ in (3.51) is to minimize the scalar $\mathbf{d}^T\mathbf{P}(t_0+(k+m)h)\mathbf{d}$, where $\mathbf{d} \in R^n$ is an arbitrary vector. Setting up this scalar and rearranging, it is seen that the minimum value is obtained, if $\mathbf{H}$ is chosen as

$$
\begin{aligned}
&\mathbf{H}(t_0+(k+m)h) \\
&= \mathbf{\Theta}(t_0+(k+m)h, t_0+kh)\mathbf{P}(t_0+kh)\mathbf{D}^T \left(\mathbf{R_e} + \mathbf{D}\mathbf{P}(t_0+kh)\mathbf{D}^T\right)^{-1}
\end{aligned}
\tag{3.56}
$$

Then the minimized value of the updated estimation error covariance matrix is

$$
\begin{aligned}
&\mathbf{P}(t_0+(k+m)h) \\
&= \mathbf{\Theta}(t_0+(k+m)h, t_0+kh)\mathbf{P}(t_0+kh)\mathbf{\Theta}^T(t_0+(k+m)h, t_0+kh) \\
&\quad - \mathbf{\Theta}(t_0+(k+m)h, t_0+kh)\mathbf{P}(t_0+kh)\mathbf{D}^T \left(\mathbf{R_e} + \mathbf{D}\mathbf{P}(t_0+kh)\mathbf{D}^T\right)^{-1} \\
&\quad \mathbf{D}\mathbf{P}(t_0+kh)\mathbf{\Theta}^T(t_0+(k+m)h, t_0+kh) \\
&\quad + \mathbf{b}_1(t_0+(k+m)h, t_0+kh)\mathbf{R}_{\ddot{\mathbf{u}}(0)}(t_0+kh)\mathbf{b}_1^T(t_0+(k+m)h, t_0+kh)
\end{aligned}
\tag{3.57}
$$

For $m = 1$, (3.58) is a difference equation which states $\mathbf{P}(t_0 + kh)$, $k = 1, .., N-1$ with the initial condition $\mathbf{P}(t_0) = \mathbf{0}$. Next, $\mathbf{P}(t_0 + (k + m)h)$ can be calculated for arbitrary k and m from (3.58).

The reconstruction defined by (3.51), (3.57) and (3.58) is called the *Kalman filter*.

The closed-loop control force $\mathbf{F}^{(c)}(t_0+(k+m)h)$ is then determined on the basis of the estimate $\hat{\mathbf{Y}}(t_0+(k+m)h)$ by

$$
\mathbf{F}^{(c)}(t_0+(k+m)h) = -\mathbf{G}\hat{\mathbf{Y}}^{(c)}(t_0+(k+m)h)
\tag{3.58}
$$

where $\mathbf{G}$ is given by (3.39).

Chapter 4

Experimental Study of Closed-Loop Control

Experiments of active control were carried out in the laboratory using a model structure under a linear closed-loop control as developed in chapters 2 and 3.

Two series of experiments were carried out :

- modal space control of free vibrations

- modal space control of forced vibrations caused by a harmonic base excitation

Initially, modal properties were identified for system identification, such as eigenfrequencies and modal damping ratios. These parameters were identified by uncontrolled, damped free vibration tests.

4.1   Experimental Setup

The model structure was mounted on a seismic simulator. Transducers measuring the structural behaviour were attached to the model. The signals from the transducers were directed to a microprocessor (a microcomputer COMPAQ portableIII$^{\text{TM}}$) which generated the signal for the control force. The control force was actually transmitted to the structure through a active mass damper using the signal generated by the microprocessor.

The model structure is a monopile with two concentrated masses, see fig. 4.1. It is made as a 4 m high box profile ($70 \times 40 \times 4$) with two concentrated masses of approximately 25 kg. The pile is bolted to a plate, called the base. This plate is fastened to two spring blades which can only move in one direction.

The forced vibrations were due to horizontal movements of the base. The movements were created by a hydraulic cylinder, Schenck, type P1 63H connected to a control system. This system provided a sinusoidal movement with a given amplitude and frequency.

Three transducers were installed on the model. A displacement transducer was installed on the base and an accelerometer was mounted on each of the concentrated masses. The signal from the displacement transducer was used directly as a measure of the displacement of the base, and it was differentiated numerically to give the velocity . The measured acceleration signals, $\ddot{Z}_1$ and $\ddot{Z}_2$, were used to determine the displacement and velocity of the two concentrated masses. This conversion was carried out by numerical integration.
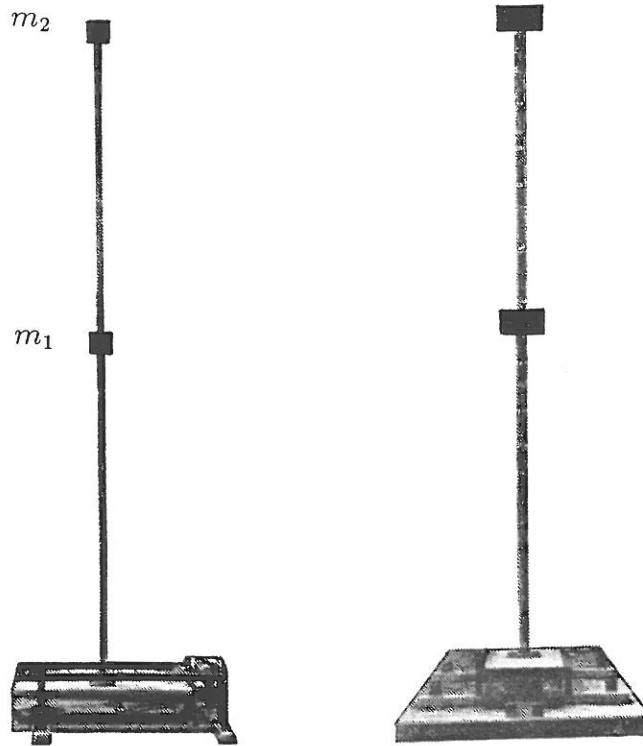
Figure 4.1: Experimental model without actuator.

On the instrumented model, an active mass damper was mounted to generate a control force. It consists of a vibration exciter, (also called a shaker), Brüel & Kjær, type 4809, and a secondary mass. The shaker and the secondary mass are placed on either side of the pile in order to avoid a considerable excentric loading.

The secondary mass is mounted on a roller bearing nearly without friction and rigidly connected with the moving element of the shaker. The maximum displacement of the moving element is 8 mm peak to peak, which is less than the maximum displacement of the roller bearing.

The secondary mass is constructed of small masses of approximately 1 kg. Then it is possible to vary the secondary mass, but in all experiments we have used 10 kg. The shaker and the secondary mass are mounted on a console, and the total weight of this system, designated m_3, is 26 kg, see fig. 4.2.

The main dimensions of the model structure and the location of the console are shown schematically in fig. 4.3.

The on-line calculations of the control algorithm were carried out by the microprocessing unit based on an COMPAQ portableIII$^{\text{TM}}$ microcomputer. The microprocessor was operated by MS-DOS 3.2 operating system and real-time processed Turbo Pascal 5.0 commands. The acquired data were transferred to the microprocessor and the computed data were transmitted to the actuator, using an analog and digital I/O board, DT2821.
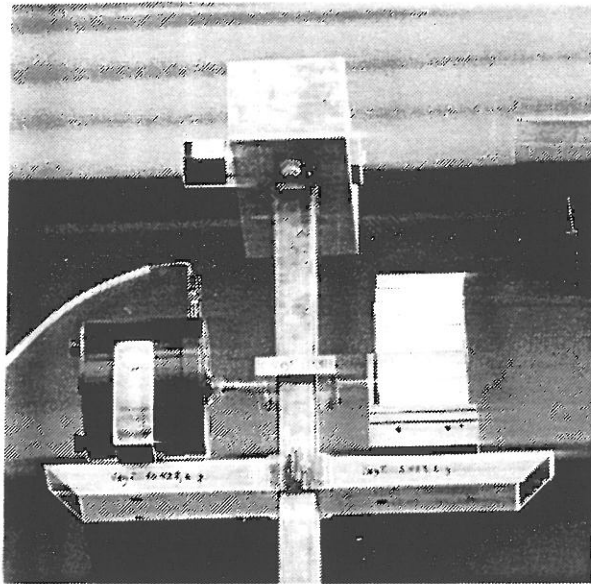
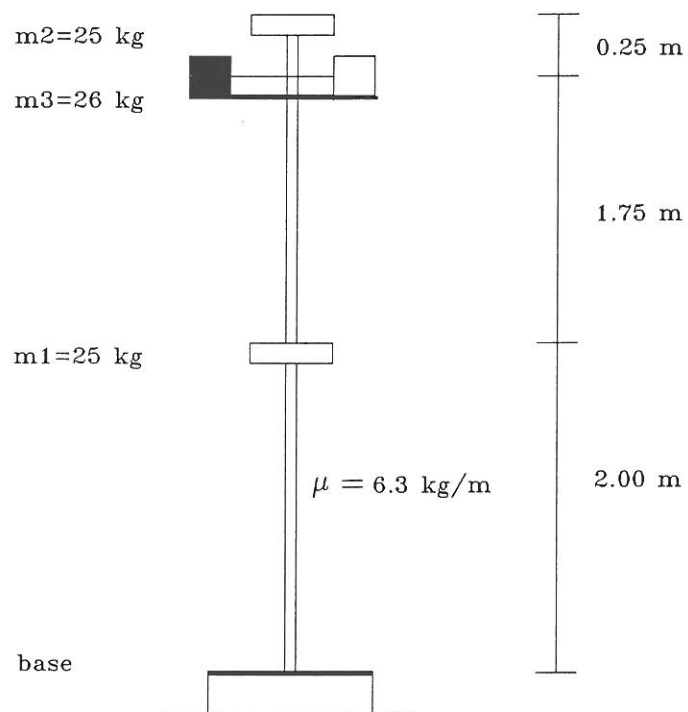Figure 4.2: Active mass damper.

Figure 4.3: Experimental model with dimensions.

4.2 Implementation of Closed-Loop Control in Modal Space

In this section the control concepts in the preceding chapters are modified for implementation in practice.

The three measured signals, two accelerations $\ddot{Z}_\alpha$, $\alpha = 1, 2$, and the base displacement $u^{(0)}$ are sampled asynchronously. The sampled version of the three signals is given by the sequences : $\{\ddot{Z}_1((3k-2)h_0), \ k = 1, 2, ..., N\}$, $\{\ddot{Z}_2((3k-1)h_0), \ k = 1, 2, ..., N\}$ and $\{u^{(0)}(3kh_0), \ k = 1, 2, ..., N\}$. h_0 is the sampling period of the serial-sampling. The sampling period defined in chapter 2 is then given by $h = 3h_0$.

The control schemes described in the preceding chapters implies that the full state vector is measured at the same time. Because of the asynchronous sampling it is not possible to determine all components in the state vector directly at the same time. Thus, the sampled signals are extrapolated to the nearest common time. The displacement of the base is sampled last, and the acceleration signals are extrapolated to that sample time by linear regression. This yields, see fig. 4.4

$$\begin{bmatrix} \ddot{Z}_1(3kh_0) \\ \ddot{Z}_2(3kh_0) \end{bmatrix} = \begin{bmatrix} \ddot{Z}_1((3k-2)h_0) + \frac{2}{3}\left(\ddot{Z}_1((3k-2)h_0) - \ddot{Z}_1((3k-5)h_0)\right) \\ \ddot{Z}_2((3k-1)h_0) + \frac{1}{3}\left(\ddot{Z}_2((3k-1)h_0) - \ddot{Z}_2((3k-4)h_0)\right) \end{bmatrix},$$
$$k = 0, 1, ..., N-1 \qquad (4.1)$$

From the extrapolated state vector, the Kalman filter is used to estimate the state vector corresponding to the time at which the control force can be applied, cf. (3.58).
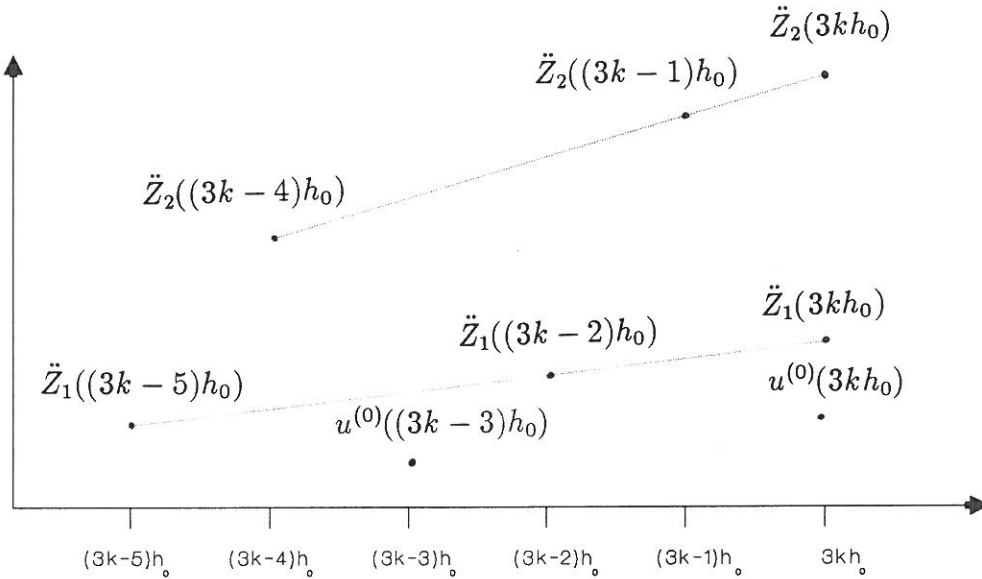

Figure 4.4: Linear extrapolation of acceleration signals.

4.2.1 Filtering and Numerical Integration of the Sampled Acceleration Signals

The mean value of the base excitation is zero and consequently, the mean value of the measured acceleration signals has to be zero since the model is linear. To ensure that the mean value criterion is fulfilled a moving average digital filter is implemented. A digital filter of order N_0 based on the extrapolated accelerations (4.1) is chosen as

$$\ddot{Z}_{\alpha,ma}(3kh_0) = \ddot{Z}_\alpha(3kh_0) - \frac{1}{N_0}\sum_{i=k-N_0+1}^{k}\ddot{Z}_\alpha(3ih_0), \ \alpha = 1, 2 \ , \quad k \geq N_0 \qquad (4.2)$$

An input sequence corresponding to about one vibration period is desired. If the period of the lowest eigenmode is designated T_1, we have

$$N_0 = \left[\frac{T_1}{3h_0} \right] \tag{4.3}$$

where $[\cdot]$ denotes Gauss' symbol. Displacements and velocities are determined by numerical integration of (4.2). Use of the trapezoidal rule yields

$$\dot{Z}_\alpha(3kh_0) = \left(\frac{1}{2}\ddot{Z}_{\alpha,ma}(0) + \frac{1}{2}\ddot{Z}_{\alpha,ma}(3kh_0) + \sum_{i=1}^{k-1} \ddot{Z}_{\alpha,ma}(3ih_0) \right) 3h_0 \quad , \\ \alpha = 1,2 \tag{4.4}$$

The velocity sequence determined from (4.4) is filtered by analogy with (4.2)

$$\dot{Z}_{\alpha,ma}(3kh_0) = \dot{Z}_\alpha(3kh_0) - \frac{1}{N_0} \sum_{i=k-N_0+1}^{k} \dot{Z}_\alpha(3ih_0), \alpha = 1,2 \ , k \geq N_0 \tag{4.5}$$

Finally, the filtered sequence $Z_{\alpha,ma}$, $\alpha = 1,2$ is determined after the same procedure as the filtered sequence $\dot{Z}_{\alpha,ma}$, $\alpha = 1,2$

The mean value of the filtered velocity sequence is not expected to be 0 until after one vibration period. Further, one vibration period will pass before the displacement sequence is expected to have zero mean, see fig. 4.5.
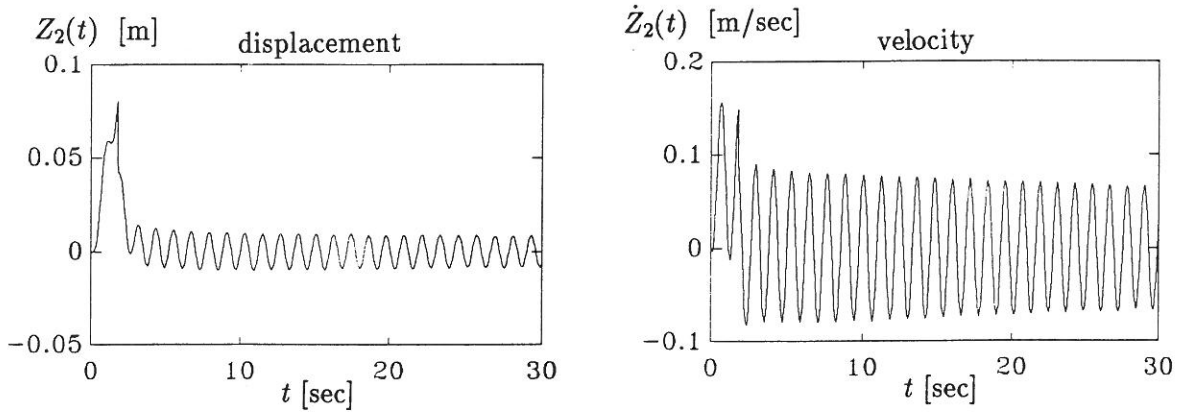

Figure 4.5: Displacement and velocity of m_2 determined by numerical integration.

The relative velocity and displacement are given by

$$\left. \begin{array}{l} v_\alpha(3kh_0) = Z_{\alpha,ma}(3kh_0) - u^{(0)}(3kh_0) \\ \dot{v}_\alpha(3kh_0) = \dot{Z}_{\alpha,ma}(3kh_0) - \dot{u}^{(0)}(3kh_0) \end{array} \right\} \ , \ k = 0,1,..,N-1 \ , \ \alpha = 1,2 \tag{4.6}$$

$\dot{u}^{(0)}(3kh)$ is determined by numerical differentiation according to

$$\dot{u}^{(0)}(3kh_0) = \frac{u^{(0)}(3kh_0) - u^{(0)}(3(k-1)h_0)}{3h_0} \tag{4.7}$$

The modal displacements and - velocities are then obtained according to (2.82) as

$$\begin{bmatrix} q_1(3kh_0) \\ q_2(3kh_0) \end{bmatrix} = [\mathbf{D}]^{-1} \begin{bmatrix} v_1(3kh_0) \\ v_2(3kh_0) \end{bmatrix} \quad , \quad k = 0,1,..,N-1 \tag{4.8}$$

$$\begin{bmatrix} \dot{q}_1(3kh_0) \\ \dot{q}_2(3kh_0) \end{bmatrix} = [\,\mathbf{D}\,]^{-1} \begin{bmatrix} \dot{v}_1(3kh_0) \\ \dot{v}_2(3kh_0) \end{bmatrix} \quad , \quad k = 0, 1, .., N-1 \tag{4.9}$$

$$\mathbf{D} = \begin{bmatrix} \Phi_1^{(1)}(l_1) & \Phi_1^{(2)}(l_1) \\ \Phi_2^{(1)}(l_2) & \Phi_2^{(2)}(l_2) \end{bmatrix} \tag{4.10}$$

4.2.2   Estimation of Modal State-Space Vector

In these experiments with active control the time delay was large compared to the sampling period $h = 3h_0$. The total time delay was mainly caused by the delay between the control signal sent off and the time, where the desired acceleration of the secondary mass was obtained. This time delay is designated mh, where m is given as

$$m = d + m_0 \;,\quad m_0 \in \,]0,1[\;,\quad d = 0, 1, 2, .. \tag{4.11}$$

In state form the modal equation for the jth mode can be expressed as, cf. (3.1) and (3.29)

$$\begin{aligned} \mathbf{Y}_j((k+m)h) = {} & \exp\left(\mathbf{A}_j(mh)\right) \mathbf{Y}_j(kh) \\ & + \int_{kh}^{(k+m)h} \exp\left(\mathbf{A}_j((k+m)h - \tau)\right) \mathbf{B}_j p_j(\tau) \mathrm{d}\tau \\ & + \int_{kh}^{(k+m)h} \exp\left(\mathbf{A}_j((k+m)h - \tau)\right) \mathbf{B}_j a_j(\tau) \mathrm{d}\tau \end{aligned} \tag{4.12}$$

$\mathbf{Y}_j$, $\mathbf{A}_j$ and $\mathbf{B}_j$ are given by (2.70), $a_j(t)$ by (2.53) and $p_j(t)$ by (2.67).

The two integrals on the right hand side of (4.12) are considered separately. The integral containing the modal control is split up. This gives

$$\begin{aligned} & \int_{kh}^{(k+m_0)h} \exp\left(\mathbf{A}_j((k+d+m_0)h - \tau)\right) \mathbf{B}_j p_j(\tau) \mathrm{d}\tau \\ & + \int_{(k+m_0)h}^{(k+d+m_0)h} \exp\left(\mathbf{A}_j((k+d+m_0)h - \tau)\right) \mathbf{B}_j p_j(\tau) \mathrm{d}\tau \end{aligned} \tag{4.13}$$

It appears from fig. 4.6 that $p_m(t)$ is constant and equal $p_m\left((k-1+m_0)h\right)$ in the interval $]kh, (k+m_0)h]$. Then the first term in (4.13) can be written as

$$\begin{aligned} & \int_{kh}^{(k+m_0)h} \exp\left(\mathbf{A}_j\left((k+d+m_0)h - \tau\right)\right) \mathbf{B}_j p_j(\tau) \mathrm{d}\tau \\ & = \mathbf{b}_{1,j}^{(0)} p_j\left(((k-1+m_0)h\right) \end{aligned} \tag{4.14}$$

where

$$\begin{aligned} \mathbf{b}_{1,j}^{(0)} & = \int_{kh}^{(k+m_0)h} \exp\left(\mathbf{A}_j\left((k+d+m_0)h - \tau\right)\right) \mathrm{d}\tau \mathbf{B}_j \\ & = \mathbf{A}_j^{-1}\left(\exp\left(\mathbf{A}_j(d+m_0)h\right) - \exp\left(\mathbf{A}_j dh\right)\right) \mathbf{B}_j \end{aligned} \tag{4.15}$$

The second term in (4.13) yields

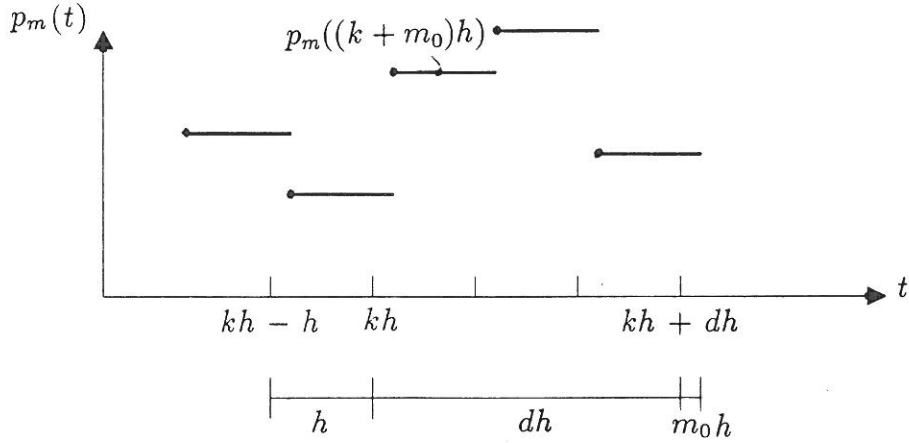$$\int_{(k+m_0)h}^{(k+d+m_0)h} \exp\left(\mathbf{A}_j\left((k+d+m_0)h - \tau\right)\right) \mathbf{B}_j p_j(\tau) \mathrm{d}\tau$$

Figure 4.6: Discrete time modal control force.

The second term in (4.13) yields

$$\int_{(k+m_0)h}^{(k+d+m_0)h} \exp\left(\mathbf{A}_j\left((k+d+m_0)h-\tau\right)\right)\mathbf{B}_j p_j(\tau)\mathrm{d}\tau$$

$$= \sum_{i=1}^{d}\int_{(k+i-1+m_0)h}^{(k+i+m_0)h} \exp\left(\mathbf{A}_j\left((k+d+m_0)h-\tau\right)\right)\mathbf{B}_j p_j(\tau)\mathrm{d}\tau$$

$$= \sum_{i=1}^{d}\mathbf{b}_{1,j}^{(i)}\; p_j\left((k+i-1+m_0)h\right) \tag{4.16}$$

where

$$\mathbf{b}_{1,j}^{(i)} = \int_{(k+i-1+m_0)h}^{(k+i+m_0)h} \exp\left(\mathbf{A}_j\left((k+d+m_0)h-\tau\right)\right)\mathrm{d}\tau \mathbf{B}_j$$

$$= \mathbf{A}_j^{-1}\left(\exp\left(\mathbf{A}_j(d-i+1)h\right) - \exp\left(\mathbf{A}_j(d-i)h\right)\right)\mathbf{B}_j \tag{4.17}$$

The last integral in (4.12) is solved in the same way, see figure 4.7

$$\int_{kh}^{(kh+d+m_0)h} \exp\left(\mathbf{A}_j\left((k+d+m)h-\tau\right)\right)\mathbf{B}_j a_j(\tau)\mathrm{d}\tau$$

$$= \mathbf{b}_{1,j}^{(0)}a_j\left((k-1+m_0)h\right) + \sum_{i=1}^{d}\mathbf{b}_{1,j}^{(i)}\; a_j\left((k+i-1+m_0)h\right) \tag{4.18}$$

Hereby, (4.12) can be written in the form

$$\mathbf{Y}_j((k+d+m_0)h) = \exp\left(\mathbf{A}_j\left((d+m_0)h\right)\right)\mathbf{Y}_j(kh)$$

$$+ \sum_{i=0}^{d}\mathbf{b}_{1,j}^{(i)}\left(p_j\left((k+i-1+m_0)h\right)\right.$$

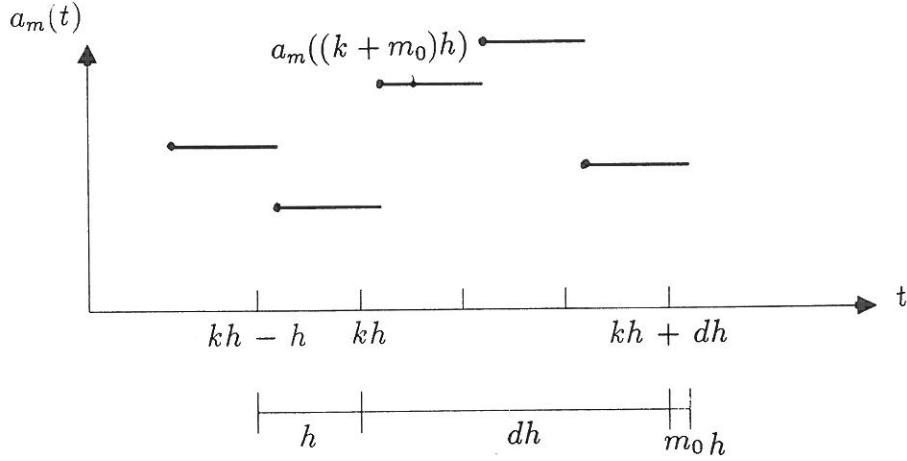$$+ \; a_j\left((k+i-1+m_0)h\right)\Bigg) \tag{4.19}$$

Figure 4.7: Discrete time modal base acceleration.

When the base excitation is harmonic $u^{(0)} = u_0^{(0)} \sin(\omega t)$, we have, cf. (2.53)

$$
\begin{aligned}
a_j(t) &= -\frac{1}{M_j} \sum_{i=1}^{3} \left(\int_0^{l_i} \left(\Phi_i^{(j)}(x_i)\mu(x_i)\frac{\partial^2}{\partial t^2}u_0^{(0)}\sin(\omega t) \right) dx_i \right. \\
&\quad + \left. \Phi^{(j)}(l_i)m_i\frac{\partial^2}{\partial t^2}u_0^{(0)}\sin(\omega t) \right) \Longrightarrow \\
a_j(kh) &= \frac{u_0^{(0)}\omega^2}{M_j}\sin(\omega kh)\sum_{i=1}^{3}\left(\int_0^{l_i}\Phi_i^{(j)}(x_i)\mu(x_i)dx_i + \Phi_i^{(j)}(l_i)m_i \right) \quad (4.20)
\end{aligned}
$$

If $a_j(t)$ instead is a white Gaussian noise, the future state is predicted on the basis of the Kalman filter (3.51),

$$
\begin{aligned}
\hat{\mathbf{Y}}_j((k+m)h|kh) &= \exp\left(\mathbf{A}_j(d+m_0)h \right)\hat{\mathbf{Y}}_j(kh|(k-1)h) \\
&\quad + \sum_{i=0}^{d}\mathbf{b}_{1,j}^{(i)}p_j\left((k+i-1+m_0)h \right) \\
&\quad + \mathbf{H}((k+m)h)\left(\mathbf{Z}(kh) - \mathbf{D}\hat{\mathbf{Y}}_j(kh|(k-1)h)) \right) \quad (4.21)
\end{aligned}
$$

$\mathbf{D}$ is given by (4.10). In the context of data acquisition, linear extrapolation and numerical integration, the measuring noise is assumed to be negligible, i.e. $\mathbf{R_e} \simeq \mathbf{0}$. Hence, the gain matrix $\mathbf{H}_j((k+m)h)$ is reduced to, cf. (3.56)

$$
\mathbf{H}_j((k+m)h) = \exp(\mathbf{A}_j(d+m_0)h)\mathbf{D}^{-1} \quad (4.22)
$$

Finally, the estimated state vector is obtained by substituting (3.41) and (4.22) into (4.21)

$$
\begin{aligned}
\hat{\mathbf{Y}}_j((k+m)h|kh) &= \exp(\mathbf{A}_j(d+m_0)h)\hat{\mathbf{Y}}_j(kh|(k-1)h) \\
&\quad + \sum_{i=0}^{d}\mathbf{b}_{1,j}^{(i)}\, p_j((k+i-1+m_0)h) \quad (4.23)
\end{aligned}
$$

4.2.3 Determination of the Control Force

For the considered closed-loop control system the Ricatti matrix is assumed to be time-independent, cf. (3.23).

Thus, the modal control force for the jth mode is given in the form, cf. (3.28)

$$p_j^{(c)}((k+m)h) = -\mathbf{G}_j \hat{\mathbf{Y}}_j^{(c)}((k+m)h|kh) \ , \quad j = 1,2 \tag{4.24}$$

where the modal gain vector in the jth mode is obtained from, cf. (3.39)

$$\mathbf{G}_j = \left(\ r_{22,j} + \mathbf{b}_{2,j}^T(h,0)\mathbf{S}_j\mathbf{b}_{2,j}(h,0)\ \right)^{-1} \left(\ \mathbf{Q}_{02,j}^T + \mathbf{b}_{2,j}^T(h,0)\mathbf{S}_j\mathbf{\Theta}_j(h,0)\ \right) \tag{4.25}$$

$\mathbf{S}_j$ is obtained from the steady-state Ricatti equation in modal space, cf. (3.38)

$$\begin{aligned}
\mathbf{S}_j =\ & \mathbf{Q}_{00,j} + \mathbf{\Theta}_j^T(h,0)\mathbf{S}_j\mathbf{\Theta}_j(h,0) - \left(\ \mathbf{Q}_{02,j} + \mathbf{\Theta}_j^T(h,0)\mathbf{S}_j\mathbf{b}_{2,j}(h,0)\ \right) \\
& \left(\ r_{22,j} + \mathbf{b}_{2,j}^T(h,0)\mathbf{S}_j\mathbf{b}_{2,j}(h,0)\ \right)^{-1} \left(\ \mathbf{Q}_{02,j}^T + \mathbf{b}_{2,j}^T(h,0)\mathbf{S}_j\mathbf{\Theta}_j(h,0)\ \right)
\end{aligned} \tag{4.26}$$

in which

$$\mathbf{\Theta}_j(h,0) = \exp(\mathbf{A}_j h) \tag{4.27}$$

$$\begin{aligned}
\mathbf{b}_{2,j}(t,kh) &= \int_{kh}^t \exp\left(\mathbf{A}_j(t-\tau)\right)\mathbf{B}_j \mathrm{d}\tau \\
&= \mathbf{A}_j^{-1}(\exp(\mathbf{A}_j(t-kh)) - \mathbf{E})\mathbf{B}_j
\end{aligned} \tag{4.28}$$

$\mathbf{A}_j$ and $\mathbf{B}_j$ are given by (2.63). $\mathbf{Q}_{00,j}$, $\mathbf{Q}_{02,j}$ and $r_{22,j}$ become, cf. (3.10), (3.14) and (3.15)

$$\mathbf{Q}_{00,j} = \int_{kh}^{(k+1)h} \mathbf{\Theta}_j^T(\tau,kh)\mathbf{Q}_j\mathbf{\Theta}_j(\tau,kh)\,\mathrm{d}\tau \tag{4.29}$$

$$\mathbf{Q}_{02,j} = \int_{kh}^{(k+1)h} \mathbf{\Theta}_j^T(\tau,kh)\mathbf{Q}_j\mathbf{b}_{2,j}(\tau,kh)\,\mathrm{d}\tau \tag{4.30}$$

$$r_{22,j} = \int_{kh}^{(k+1)h} \left(\mathbf{b}_{2,j}^T(\tau,kh)\mathbf{Q}_j\mathbf{b}_{2,j}(\tau,kh) + r_j\right)\mathrm{d}\tau \tag{4.31}$$

The modal weighting matrix $\mathbf{Q}_j$ is chosen as (2.66).

The modal weighting factor r_j for the jth mode is assumed to be time-invariant. As r_j increases, more weight is placed on the control energy in the performance index (2.65) and hence, the control force decreases. Then r_j has to be chosen in proportion to the available control force. In figure 4.8 the gain factors $g_{1,1}$ and $g_{2,1}$ are illustrated as functions of r_1. The values on the abscissa are those which are relevant in the experiments.
On the basis of the estimated modal state vector the energy level in each mode is calculated according to (2.80). Then the mode with the highest energy level is controlled.

From the modal control force given by (4.24) the physical control force is calculated from (2.54). Since only one actuator is implemented, the physical control force is given by

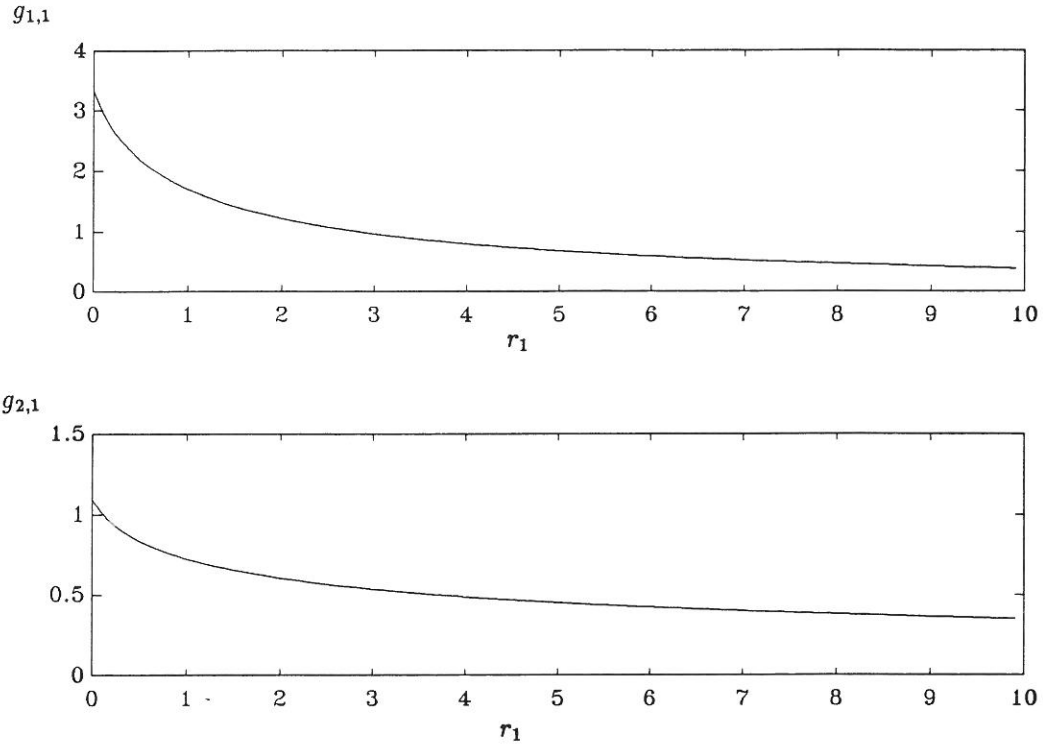$$F^{(c)}(kh) = \frac{p_j^{(c)}(kh)M_j}{\Phi_3^{(j)}(l_3)} \ , \quad k = 0,1,..,N-1 \tag{4.32}$$

Figure 4.8: Gain factors as a function of r_1.

4.3 System Identification

4.3.1 Determination of Dynamic Parameters

The dynamic parameters of the model structure were identified experimentally for the two lowest modes in the direction of the excitation.

The dynamic properties are determined for the distributed parameter model shown in fig.4.3.

A free vibration test was carried out for the first and second mode, respectively. In each test the base was subjected to a sine excitation with constant amplitude and with a frequency implying resonance in the model. When resonance was obtained the excitation was stopped and subsequently, the acceleration of the free vibration was measured.

The damping ratio is determined from the logarithmic decrement δ given by

$$\delta = \frac{1}{N_1} \ln \left(\frac{a_1}{a_2} \right) \tag{4.33}$$

N_1 is the number of cycles, a_1 and a_2 are the amplitudes for the first and last oscillation within the considered periods.

The damping ratio in the jth mode, ζ_j, is then determined from the associated logarithmic decrement δ_j as

$$\zeta_j = \frac{\frac{\delta_j}{2\pi}}{\sqrt{1 - \left(\frac{\delta_j}{2\pi} \right)^2}} \quad , \quad j = 1, 2 \tag{4.34}$$

ζ_1	ζ_2
0.0014	0.0050

Table 4.1: Modal damping ratios determined from the logarithmic decrement.

The estimated modal damping ratios are given in table 4.1.

The eigenfrequencies in the two lowest modes, f_1 and f_2, were estimated on the basis of two identification methods. Firstly, they were estimated by determination of the average frequency of the sampled acceleration signals. Secondly, the power spectral density of the sampled acceleration signals were estimated and the eigenfrequencies were obtained by reading the spectral peaks.

The estimated eigenfrequencies are given in table 4.2.

	$f_1\ [Hz]$	$f_2\ [Hz]$
Free vibration frequency	0.83	7.17
Spectral peaks	0.84	7.16

Table 4.2: Experimentally determined eigenfrequencies.

4.3.2 Determination of Modal Parameters

The eigenmodes $\Phi^{(1)}(x)$ and $\Phi^{(2)}(x)$ are determined theoretically on the basis of the Bernoulli-Euler beam theory.
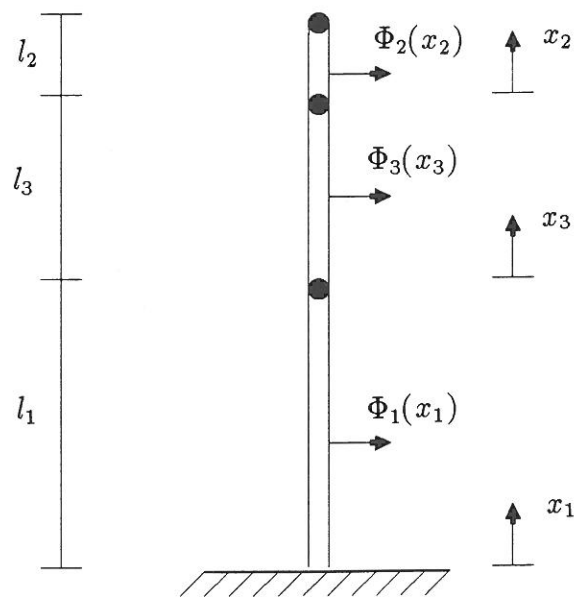

Figure 4.9: Mathematical model of the structural model.

The eigenmodes are composed of three parts, Φ_1, Φ_2 and Φ_3 belonging to the discrete

beams with length l_1, l_2 and l_3, respectively, see fig. 4.9. According to the Bernoulli-Euler theory neglecting the influence of the axial force the eigenmodes are obtained as solutions of the following differential equations

$$\frac{d^4\Phi}{dx_i^4} - \frac{\lambda_i^4}{l_i^4}\Phi_i^4 = 0 \; , \quad i = 1,2,3 \tag{4.35}$$

where

$$\lambda_i^4 = \frac{\mu\omega^2 l_i^4}{EI} \; , \quad i = 1,2,3 \tag{4.36}$$

The solutions of (4.35) are given in the form

$$\begin{aligned}
\Phi_i(x_i) &= A_i \sin\lambda_i\frac{x_i}{l_i} + B_i \cos\lambda_i\frac{x_i}{l_i} \\
&+ C_i \sinh\lambda_i\frac{x_i}{l_i} + D_i \cosh\lambda_i\frac{x_i}{l_i} \; , \quad i = 1,2,3
\end{aligned} \tag{4.37}$$

The solutions (4.37) must fulfil given boundary conditions, which results in a homogeneous system of equations for determination of the unknown constants,

$$\mathbf{L}(\omega)\mathbf{\Upsilon} = \mathbf{0} \tag{4.38}$$

where

$$\mathbf{\Upsilon}^T = [A_1, B_1, C_1, D_1, A_2, B_2, C_2, D_2, A_3, B_3, C_3, D_3] \tag{4.39}$$

Non-trivial solutions of (4.38) exist for discrete values of ω, for which the determinant of the coefficient matrix $\mathbf{L}(\omega)$ is equal 0. This leads to the frequency condition

$$\det(\mathbf{L}(\omega)) = 0 \tag{4.40}$$

For each solution $\omega_1 \leq \omega_2 \leq \cdots$ to (4.40) solutions $\mathbf{\Upsilon}^{(1)}, \mathbf{\Upsilon}^{(2)}, \dots$ of (4.39) exist. Thus, the eigenmodes are determined by inserting the coefficients into (4.37).
The modal mass for the jth mode is obtained from

$$M_j = \sum_{i=1}^{3}\left(\int_0^{l_i}\left(\Phi_i^{(j)}(x_i)\right)^2\mu(x_i)dx_i + \left(\Phi_i^{(j)}(l_i)\right)^2 m_i \right), j = 1,2 \tag{4.41}$$

corresponding to (2.51).

4.4 Experimental Results

The experiments are as previously mentioned split up into active control of free and forced vibrations, respectively. The forced vibrations are only caused by harmonic excitations in the range of the eigenfrequency in the first mode. This implies, that the modal coordinates in the second mode are small compared to those of the first mode. Naturally, the system is dominated by the modal energy level in the first mode.

The control force is applied at time $t = 3$ sec. to ensure, that the mean value of the velocities and the displacements determined by numerical integration is equal 0.

In all experiments the sampling frequency is 60 Hz, i.e. 20 Hz for each signal.
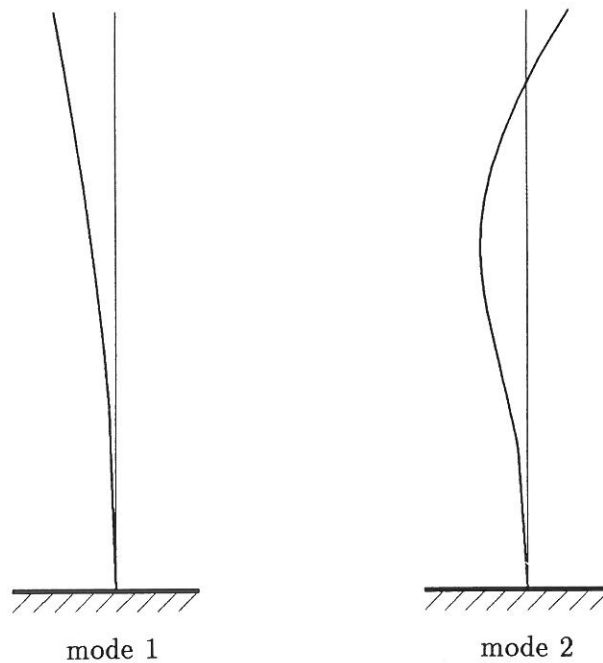
mode 1   mode 2

Figure 4.10: 1st and 2nd eigenmode.

	r_1	g_1	g_2
Test 1	1.02	1.69	0.72

Table 4.3: Weighting factor and corresponding gain factors (test 1).

4.4.1 Active Control of Free Vibrations

The free vibrations were caused by an initial displacement of the model top in about 25 mm. After 3 sec. the control force was calculated as described in section 4.2 and applied to the structure. Fig. 4.11 shows the sampled acceleration signal of m_2

The chosen r_1-value and the associated gain factors are written in table 4.3

In table 4.4 the controlled natural frequency f and the controlled damping factor ζ are stated. It is seen, that the damping factor is increased considerably compared to the damping ratio in the first mode, but there is only a slight increase in the natural frequency compared to the eigenfrequency in the first mode, see table 4.1.

	f [Hz]	ζ
Test 1	0.86	0.022

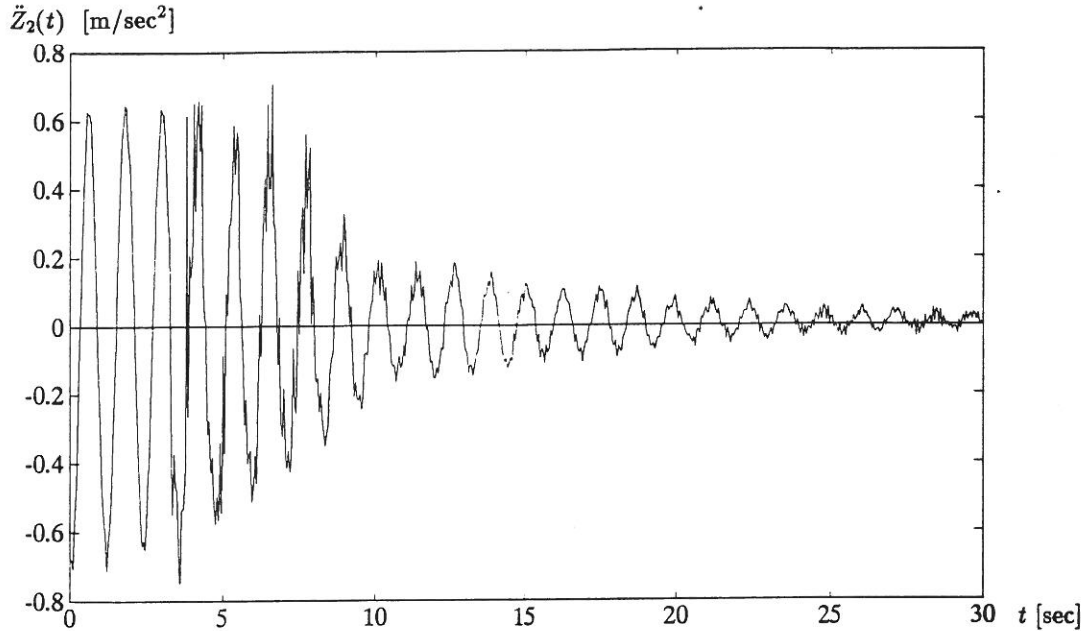Table 4.4: Frequency and damping factor of controlled vibration.

Figure 4.11: Acceleration of m_2 (test 1).

4.4.2 Active Control of Forced Vibrations.

The forced vibration is caused by a sinusoidal base excitation with a frequency f of 0.83 Hz and an amplitude $u_0^{(0)}$ of approximately 0.5 mm. The control system is activated when the vibration is stationary, i.e. the effects of the initial conditions are damped out.

The control force is calculated according to the independent modal space control scheme described in section 1.2.3.

The controlled acceleration signals of m_2 are shown in fig. 4.12 and 4.13 for two different values of the weighting factor r_1, see table 4.5. They are referred to as test 2 and 3, respectively.

	r_1	g_1	g_2
Test 2	0.61	2.05	0.81
Test 3	0.43	2.31	0.87

Table 4.5: Weighting factor and associated gain factors by forced harmonic vibrations.

Test 2 shows, that full damping of the model is obtained after 23 sec. Afterwards, the movement increases again. This is an example of the fact, that closed-loop control is not necessarily optimal. When the model movement is damped, the calculated control force is zero, but since the structure is still subjected to a base excitation, the movement increases again. Then the control force will increase too, and suppress the movement once again when the phase is correct . In test 3 where the gain factors are increased the described effect is not obtained during the considered control period. Apparently, the movement is damped more slowly, which is not in accordance with the employed theory. This is due to the phenomenon that more time is used before the control force obtains the correct phase in proportion to the model vibrations in test 3 than in test 2. This is illustrated in fig. 4.14 and fig. 4.15.

The maximum control force applied to the structure is approximately 0.9 N, while the

$\ddot{Z}_2(t)$ [m/sec^2]
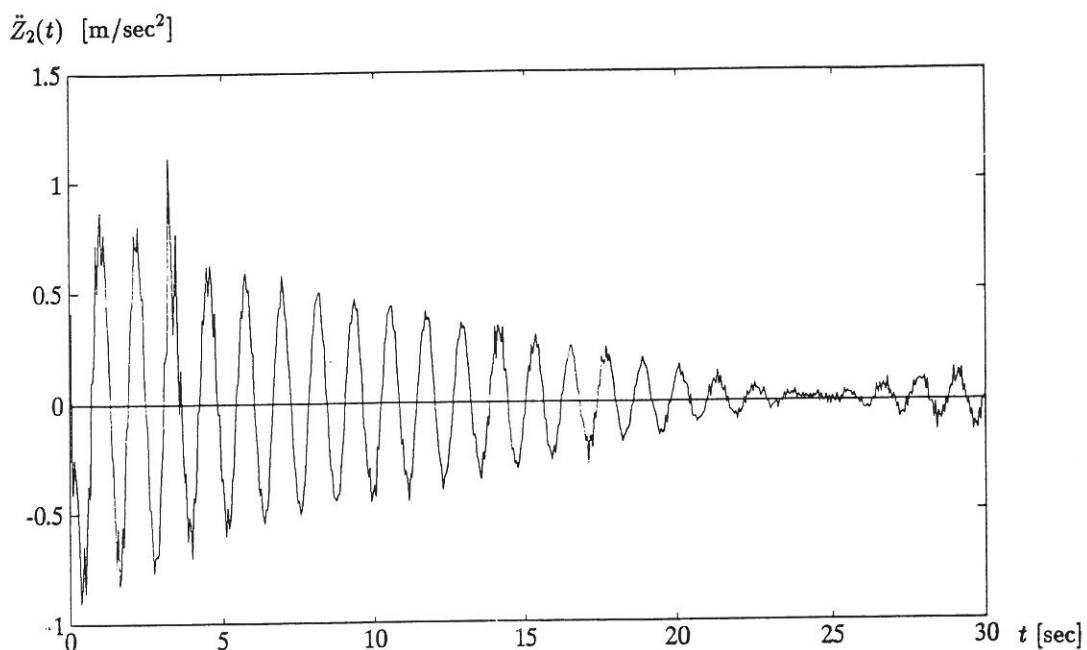
Figure 4.12: Acceleration of m_2 (test 2).

$\ddot{Z}_2(t)$ [m/sec^2]
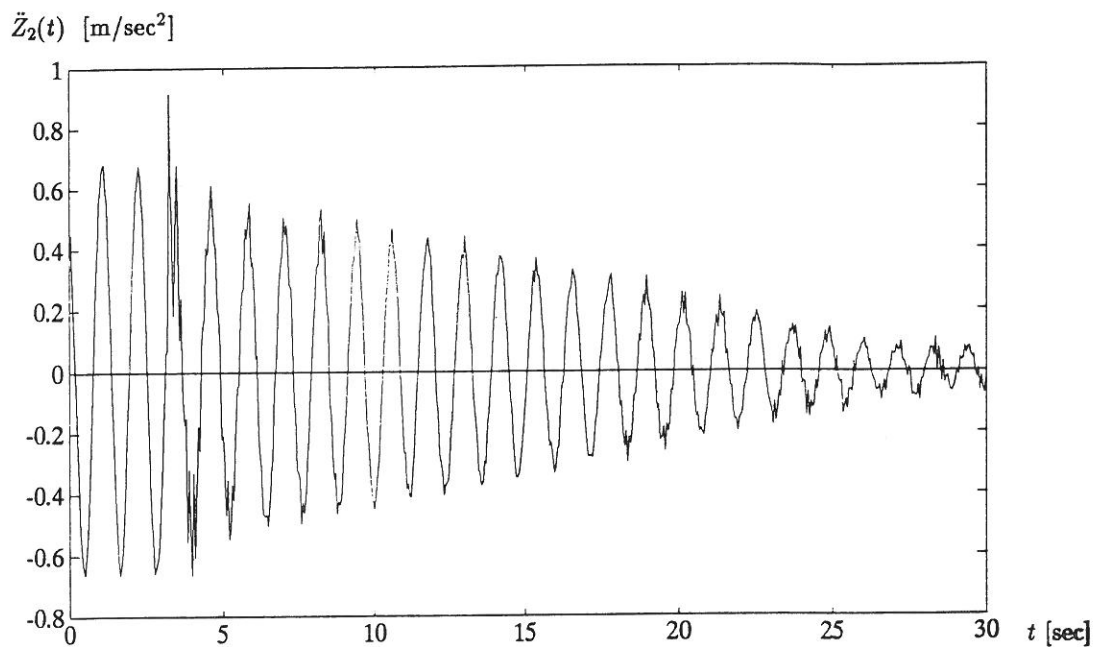
Figure 4.13: Acceleration of m_2 (test 3).

maximum available control force is

$$
\begin{aligned}
F_{max} &= a_s \omega_1^2 m_m = 0.004 \text{ m} \cdot (5.21)^2 \text{sec}^{-2} \cdot 10 \text{ kg} \\
&= 1.08 \text{ N}
\end{aligned}
$$

a_s is the maximum amplitude of the moving element in the shaker, and m_m is the vibrated mass.

$F^{(c)}(t)$ [N]

Figure 4.14: Control force (test 2).

$F^{(c)}(t)$ [N]

Figure 4.15: Control force (test 3).
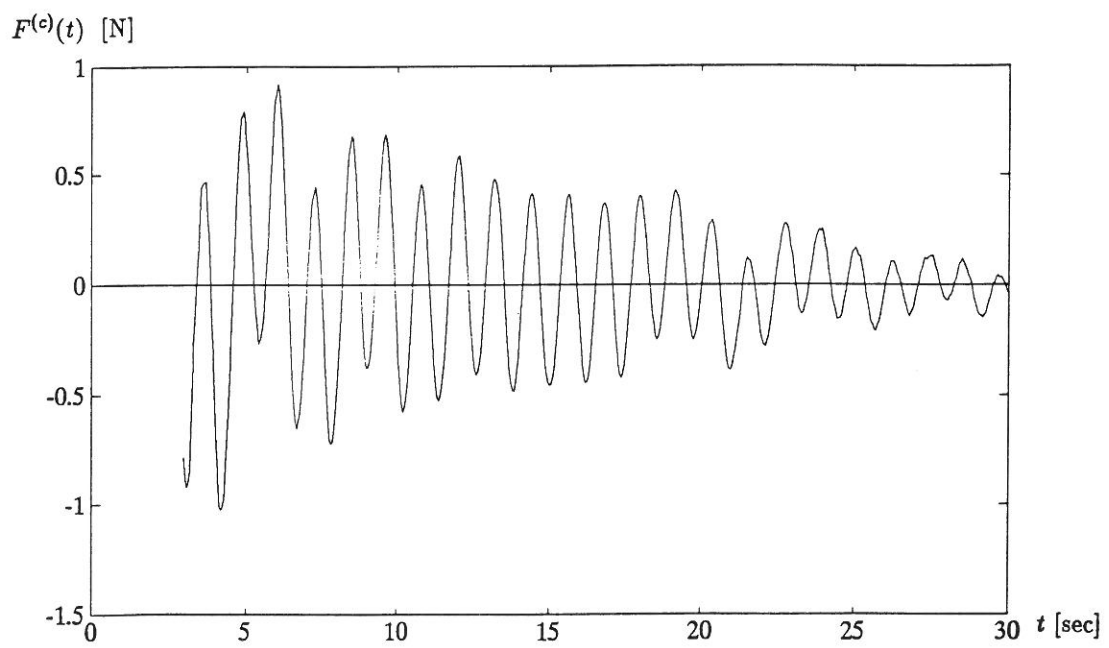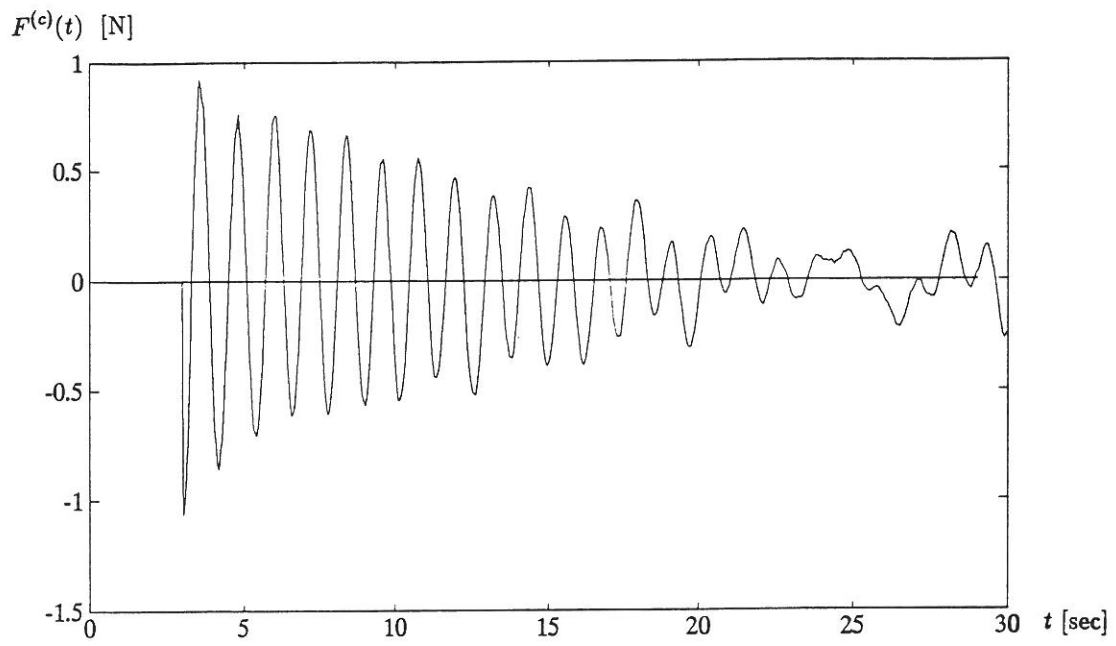
Chapter 5

Summary and Concluding Remarks

Active structural control of building structures subjected to earthquake excitations has been studied. Using the classical quadratic performance index a control algorithm is investigated for a discretized and a reduced-order model, respectively. The obtained control law is composed of a closed-loop and an open-loop part. If the external loading is zero or if it can be described by a white Gaussian noise, the open-loop part is zero. Although the external loading does not fulfil these conditions the open-loop part is neglected. However, in order to determine the open-loop part one has to know the external loading history during the control period before the control system is activated, which is not realistic in practice.

Implementation of the developed control schemes in practice requires a discrete-time control algorithm. It is investigated including the effects of measuring noise and time delay between measuring and application of control forces. The feedback forces are then determined from an estimate of the state vector given by a Kalman filter.

Active structural control with a closed-loop control algorithm has been carried out experimentally, where the control algorithm was based on the described independent modal space control device. The experiments were performed using a cantilever column with two concentrated masses and a mass damper. Closed-loop control was carried out for a free vibration of the model, and for the case where it was subjected to a harmonic base excitation. Results of the experiments clearly showed that the designed control system was able to damp the vibrations of the model structure.

After carrying out the free vibration test, it was found that there was only a slight increase in the natural frequency (stiffness) for the controlled mode but the associated damping factor was increased from 0.14% to 2.2%. The slight increase in the natural frequency is caused by the chosen value of the weighting factor and with this the feedback gains.

As expected, the forced vibration tests showed that closed-loop control is not optimal. When the vibration was damped the model began moving again, since the control force is negligible in the damped system. This effect can only be eliminated by including the open-loop control force.

In all the experimental tests the vibration is first damped out about 20 sec. after the control system has been activated. To minimize this time period it is necessary to optimize the weighting coefficients in proportion to the available maximum control forces.

45

Further studies of active control will concentrate on improving the control algorithms when the structure is subjected to an unknown external loading and optimization of the weighting coefficients.

Bibliography

[1] Chung, L.L., Reinhorn, A.M. and Soong, T.T. : "Experiments on active control of seismic structures," *Journal of Engineering Mechanics,* ASCE, Vol. 114, No. 2, pp. 241-256, Febr., 1988.

[2] Chung, L.L., Soong, T.T. and Reinhorn, A.M. : "Experimental study of active control for MDOF seismic structures," *Journal of Engineering Mechanics,* ASCE, Vol. 115, No. 8, pp. 1609-1627, 1989.

[3] Abdel-Rohman, M. and Leipholz, H.H. : "Active control of tall buildings," *Journal of Structural Engineering,* Vol. 109, No. 3, pp. 628-645, 1983.

[4] Samali, B., Yang, J.N. and Liu, S.C. : "Active control of seismic-excited buildings," *Journal of Structural Engineering,* Vol. 111, No. 10, pp. 2165-2180, 1985.

[5] Yang, J.N., Akbarpour, A. and Ghaemmaghami, P. : "New optimal control algorithms for structural control," *Journal of Engineering Mechanics,* ASCE, Vol. 113, No. 9, pp. 1369-1386, Sept., 1987.

[6] Miller, R.K., Masri, S.F., Dehghanyar, T.J. and Caughey, T.K. : "Active vibration control of large civil structures," *Journal of Engineering Mechanics,* ASCE, Vol. 114, No. 9, pp. 1542-1570, Sept., 1988.

[7] Pu, Jun-Ping and Hsu, Deh-Shiu : "Optimal control of tall buildings," *Journal of Engineering Mechanics,* Vol. 114, No. 6, pp. 973-989, 1988.

[8] Sadek, I.S., Adali, S., Sloss, J.M. and Bruch, J.C. Jr. : "Optimal distributed control of continuous beam with damping," *Journal of Sound and Vibration,* Vol. 117, No. 2, pp. 207-218, 1987.

[9] Sadek, I.S., Bruch, J.C. Jr., Sloss, J.M. and Adali, S. : "Structural control of a variable cross-section beam by distributed forces," *Mechanics of Structures and Machines,* Vol. 16, No. 3, pp. 313-333, 1988-89.

[10] Luzzato, E. and Jean, M. : "Mechanical analysis of active vibration damping in continuous structures," *Journal of Sound and Vibration,* Vol. 86, No. 4, pp. 455-473, 1983.

[11] Sadek, I.S. and Adali, S. : "Control of the dynamic response of a damped menbrane by distributed forces," *Journal of Sound and Vibration,* Vol. 96, No. 3, pp. 391-406, 1984.

[12] Meirovitch L. and Baruh, H. : "Control of self-adjoint distributed-parameter system," *Journal of Guidance and Control,* Vol. 5, No. 1, pp. 59-66, 1980.

[13] Meirovitch, L., Baruh, H. and Öz, H. : "A comparison of control techniques for large flexible systems," *Journal of Guidance and Control,* Vol. 6, No. 4, pp. 302-310, 1983.

[14] O'Donoghue, P.E. and Atluri, S.N. : "Control of dynamic response of a continuum model of a large space structure," *Computers & Structures,* Vol. 23, No. 2, pp. 199-209, 1986.

[15] Baz, A. and Poh, S. : "Performance of an active control system with piezoelectric acturators," *Journal of Sound and Vibration,* Vol. 126, No. 2, pp. 327-343, 1988.

[16] Baz, A. and Poh, S. : "Experimental implementation of the modified independent modal space control method," *Journal of Sound and Vibration,* Vol. 139, No. 1, pp. 133-149, 1990.

[17] Bryson, E.A. Jr. : *Applied Optimal Control,* John Wiley & Sons, Inc., 1975.

[18] Lewis, Frank. L. : *Optimal Control,* John Wiley & Sons, Inc., 1986.

[19] Åström, K.J and Wittenmark, B. : *Computer Controlled Systems; Theory and Design,* Prentice-Hall, Inc., 1984.

[20] Brogan, W.L. : *Modern Control Theory,* Prentice-Hall, Inc., 1985.

FRACTURE AND DYNAMICS PAPERS

PAPER NO. 1: J. D. Sørensen & Rune Brincker: *Simulation of Stochastic Loads for Fatigue Experiments*. ISSN 0902-7513 R8717.

PAPER NO. 2: R. Brincker & J. D. Sørensen: *High-Speed Stochastic Fatigue Testing*. ISSN 0902-7513 R8809.

PAPER NO. 3: J. D. Sørensen: *PSSGP: Program for Simulation of Stationary Gaussian Processes*. ISSN 0902-7513 R8810.

PAPER NO. 4: Jakob Laigaard Jensen: *Dynamic Analysis of a Monopile Model*. ISSN 0902-7513 R8824.

PAPER NO. 5: Rune Brincker & Henrik Dahl: *On the Fictitious Crack Model of Concrete Fracture*. ISSN 0902-7513 R8830.

PAPER NO. 6: Lars Pilegaard Hansen: *Udmattelsesforsøg med St. 50-2, serie 1 - 2 - 3 - 4*. ISSN 0902-7513 R8813.

PAPER NO. 7: Lise Gansted: *Fatigue of Steel: State-of-the-Art Report*. ISSN 0902-7513 R8826.

PAPER NO. 8: P. H. Kirkegaard, I. Enevoldsen, J. D. Sørensen, R. Brincker: *Reliability Analysis of a Mono-Tower Platform*. ISSN 0902-7513 R8839.

PAPER NO. 9: P. H. Kirkegaard, J. D. Sørensen, R. Brincker: *Fatigue Analysis of a Mono-Tower Platform*. ISSN 0902-7513 R8840.

PAPER NO. 10: Jakob Laigaard Jensen: *System Identification1: ARMA Models*. ISSN 0902-7513 R8908.

PAPER NO. 11: Henrik Dahl & Rune Brincker: *Fracture Energy of High-Strength Concrete in Compression*. ISSN 0902-7513 R8919.

PAPER NO. 12: Lise Gansted, Rune Brincker & Lars Pilegaard Hansen: *Numerical Cumulative Damage: The FM-Model*. ISSN 0902-7513 R8920.

PAPER NO. 13: Lise Gansted: *Fatigue of Steel: Deterministic Loading on CT-Specimens*.

PAPER NO. 14: Jakob Laigaard Jensen, Rune Brincker & Anders Rytter: *Identification of Light Damping in Structures*. ISSN 0902-7513 R8928.

PAPER NO. 15: Anders Rytter, Jakob Laigaard Jensen & Lars Pilegaard Hansen: *System Identification from Output Measurements*. ISSN 0902-7513 R8929.

FRACTURE AND DYNAMICS PAPERS

PAPER NO. 16: Jens Peder Ulfkjær: *Brud i beton - State-of-the-Art. 1. del, brudforløb og brudmodeller*. ISSN 0902-7513 R9001.

PAPER NO. 17: Jakob Laigaard Jensen: *Full-Scale Measurements of Offshore Platforms*. ISSN 0902-7513 R9002.

PAPER NO. 18: Jakob Laigaard Jensen, Rune Brincker & Anders Rytter: *Uncertainty of Modal Parameters Estimated by ARMA Models*. ISSN 0902-7513 R9006.

PAPER NO. 19: Rune Brincker: *Crack Tip Parameters for Growing Cracks in Linear Viscoelastic Materials*. ISSN 0902-7513 R9007.

PAPER NO. 20: Rune Brincker, Jakob L. Jensen & Steen Krenk: *Spectral Estimation by the Random Dec Technique*. ISSN 0902-7513 R9008.

PAPER NO. 21: P. H. Kirkegaard, J. D. Sørensen & Rune Brincker: *Optimization of Measurements on Dynamically Sensitive Structures Using a Reliability Approach*. ISSN 0902-7513 R9009.

PAPER NO. 22: Jakob Laigaard Jensen: *System Identification of Offshore Platforms*. ISSN 0902-7513 R9011.

PAPER NO. 23: Janus Lyngbye & Rune Brincker: *Crack Length Detection by Digital Image Processing*. ISSN 0902-7513 R9018.

PAPER NO 24: Jens Peder Ulfkjær, Rune Brinker & Steen Krenk: *Analytical Model for Complete Moment-Rotation Curves of Concrete Beams in bending*. ISSN 0902-7513 R9021.

PAPER NO 25: Leo Thesbjerg: *Active Vibration Control of Civil Engineering Structures under Earthquake Excitation*. ISSN 0902-7513 R9027.

PAPER NO. 26: Rune Brincker, Steen Krenk & Jakob Laigaard Jensen: *Estimation of correlation Functions by the Random Dec Technique*. ISSN 0902-7513 R9028.